



Synthesis of sorafenib analogues incorporating a 1,2,3-triazole ring and cytotoxicity towards hepatocellular carcinoma cell lines

Sarinya Palakhachane^a, Yuwaporn Ketkaew^b, Natthaya Chuaypen^b, Jitnapa Sirirak^a, Jutatip Boonsombat^c, Somsak Ruchirawat^{c,d}, Pisit Tangkijvanich^b, Apichart Suksamrarn^e, Panupun Limpachayaporn^{a,*}

^a Department of Chemistry, Faculty of Science, Silpakorn University, Nakhon Pathom 73000, Thailand

^b Center of Excellence in Hepatitis and Liver Cancer, Department of Biochemistry, Faculty of Medicine, Chulalongkorn University, Bangkok 10330, Thailand

^c Chulabhorn Research Institute, Bangkok 10210, Thailand

^d Chulabhorn Graduate Institute, Chemical Biology Program, Chulabhorn Royal Academy, Kamphaeng Phet 6 Road, Bangkok 10210, Thailand

^e Department of Chemistry and Center of Excellence for Innovation in Chemistry, Faculty of Science, Ramkhamhaeng University, Bangkok 10240, Thailand

ARTICLE INFO

Keywords:

Multi-kinase inhibitor
Triazole
1,3-Dipolar cycloaddition
Sorafenib analogue
Hepatocellular carcinoma (HCC)

ABSTRACT

A series of 1,2,3-triazole-containing Sorafenib analogues, in which the aryl urea moiety of Sorafenib (**1**) was replaced with a 1,2,3-triazole ring linking a substituted phenoxy fragment, were prepared successfully via Huisgen 1,3-dipolar cycloaddition and nucleophilic aromatic substitution. The studies of cytotoxicity towards human hepatocellular carcinoma (HCC) cell lines, HepG2 and Huh7, indicated that *p*-*tert*-butylphenoxy analogue **2m** showed significant inhibitory activity against Huh7 with $IC_{50} = 5.67 \pm 0.57 \mu\text{M}$. More importantly, **2m** showed low cytotoxicity against human embryonal lung fibroblast cell line, MRC-5, with $IC_{50} > 100 \mu\text{M}$, suggesting its highly selective cytotoxic activity ($SI > 17.6$) towards Huh7 which is much superior to that of Sorafenib ($SI = 6.73$). The molecular docking studies revealed that the analogue **2m** bound B-RAF near the binding position of Sorafenib, while it interacted VEGFR2 efficiently at the same binding position of Sorafenib. However, **2m** exhibited moderate inhibitory activity toward B-RAF, implying that its anti-Huh7 effect might not strictly relate to inhibition of B-RAF. Wound healing and BrdU cell proliferation assays confirmed anti-cell migration and anti-cell proliferative activities towards Huh7. With its inhibitory efficiency and high safety profile, **2m** has been identified as a promising candidate for the treatment of HCC.

1. Introduction

Hepatocellular carcinoma (HCC) is one of the most common causes of cancer death in the world [1,2] and tend to continuously rise. In 2018, HCC ranked fifth in global cancer cases and ninth in cause of death in men, while ranked second and sixth, respectively, in women [1]. HCC can be caused by several factors, from both behavior and other diseases, including alcoholism [3,4], unbeneficial eating [5], over of body mass index (BMI) [6], chronic hepatitis B and C virus infection [4,7], fibrosis and cirrhosis [8,9]. There are many treatment options for HCC, consisted of curative resection, liver transplantation (LT), radiofrequency ablation, transarterial chemoembolization and radioembolization [10], depending on the states of cancer, patient readiness and severity of liver function [11–13]. However, most of the HCC patients are diagnosed in the late stages, which are malignant phases and in metastasis [14,15].

Therefore, they usually are unable to be treated efficiently, and thus suffer from severe adverse effects of the treatments. Nowadays, the patients can be treated with targeted cancer drug therapy [12], which inhibits cancerous cells selectively without affecting normal cells resulting in less side effects and prolong of the patient's life [11].

The first targeted cancer drug for HCC patients is Sorafenib (Nexavar®). It was approved by Food and Drug Administration of the United States (US FDA) for the treatment of renal cell carcinoma (RCC) in 2005 [16,17], advanced HCC in 2007 [16,17] and thyroid cancer in 2013 [17]. Sorafenib can be used for the treatment of various cancers due to its multi-kinase inhibitory properties in various pathways associated with cancer development, especially vascular endothelial growth factor receptor (VEGFR) [18], serine/threonine protein kinase (B-RAF), Ras protein and Ras-mutation [15] and downstream of mitogen-activated protein kinase (MAPK) pathway [18,19]. These inhibitory properties

* Corresponding author.

E-mail addresses: limpachayaporn.p@silpakorn.edu, panupun.lim@gmail.com (P. Limpachayaporn).

<https://doi.org/10.1016/j.bioorg.2021.104831>

Received 17 September 2020; Received in revised form 28 February 2021; Accepted 12 March 2021

Available online 17 March 2021

0045-2068/© 2021 Elsevier Inc. All rights reserved.

lead to suppression of cell growth, angiogenesis and cell proliferation [20]. The proper interactions between Sorafenib, and B-RAF and VEGFR2 have been explained by X-ray co-crystal structure [21]. However, Sorafenib exhibits low bioavailability causing usage of high dose [22]. In addition, the broad kinase inhibition also causes strong adverse effects as reported by the FDA, such as dermatitis rash, hand-foot skin reaction, diarrhea, fatigue and hypertension [23]. Although the HCC patients may afford the treatment with Sorafenib, their life can be prolonged up to only almost a year [11]. Consequently, besides Sorafenib, the more effective and safer targeted drugs are still in need for HCC treatment.

The disclosure of the structure and cancer inhibitory properties of Sorafenib has opened the opportunities not only to improve the inhibitory efficiency, pharmacokinetic and safety profiles, but also to discover the activities against various cancer cell lines other than HCC cell lines. Thus, many organic and medicinal chemists are searching intensively for appropriate structures, analogous to the Sorafenib structure, which can potentially suppress the progression of cancers. Modification of Sorafenib's structure might be classified roughly into three groups (Fig. 1): 1) Introduction of halogen atom such as chlorine and fluorine to the core benzene [24]. These analogues were often active against the hepatocyte growth factor receptor (c-MET, also known as tyrosine-protein kinase MET) pathway, VEGFR1, VEGFR2, VEGFR3 and platelet-derived growth factor receptor- β (PDGFR β).; 2) Replacement of picolinamide with trifluoromethyl imidazole [25], indazole ring [26], thieno[3,2-*d*]pyrimidine [27] and 1,2,4-triazole [28]. They inhibited MDA-MB-231, SMMC-7721, H460, HT-29 comparable to or better than Sorafenib; 3)

Replacement of aryl urea with 4,5-dihydro-1*H*-pyrazole [29], pyrazole [30], chalcone [31]. They showed similar to superior inhibition against receptor tyrosine kinases (RTKs), VEGFR2, HepG2, MCF-7 and PC-3 when compared to Sorafenib. They are also promoting apoptosis of cancer cells. From the previous works, the Sorafenib derivatives exhibited broad inhibition towards various cancer cell lines. However, only limited number of the derivatives have been tested against HCC cell lines and showed good inhibitory activities. Nevertheless, these structural alterations originated from Sorafenib leads to the discovery of drugs for HCC treatment including Regorafenib, Lenvatinib and Tivozanib [24] (Fig. 1). Moreover, Regorafenib and Lenvatinib were approved by US FDA for the treatment of colorectal cancer [32] and differentiated thyroid cancer [33] respectively, while Tivozanib was approved in European Union (EU) for treatment of RCC [34].

According to the structure-activity relationship (SAR) investigation and molecular docking studies of the previous reports, aryl urea provided important binding interactions through the hydrogen bond with Asp, Glu and Cys, and hydrophobic interactions with the lipophilic pocket of the VEGFR2 and B-RAF [35]. Therefore, most Sorafenib analogues usually contained aryl urea moiety which provides a good affinity to the targets leading to inhibitory activities towards a broad spectrum of cancer cell lines. However, the urea-containing drug was often aggregated itself [36] and its hydrogen bond character also increased interaction with various plasma proteins [36,37], incurring poor pharmacokinetic properties and cell toxicity. Replacement of aryl urea of Sorafenib with other suitable moiety is a challenging approach since the loss of hydrogen bonding due to the absence of aryl urea would require

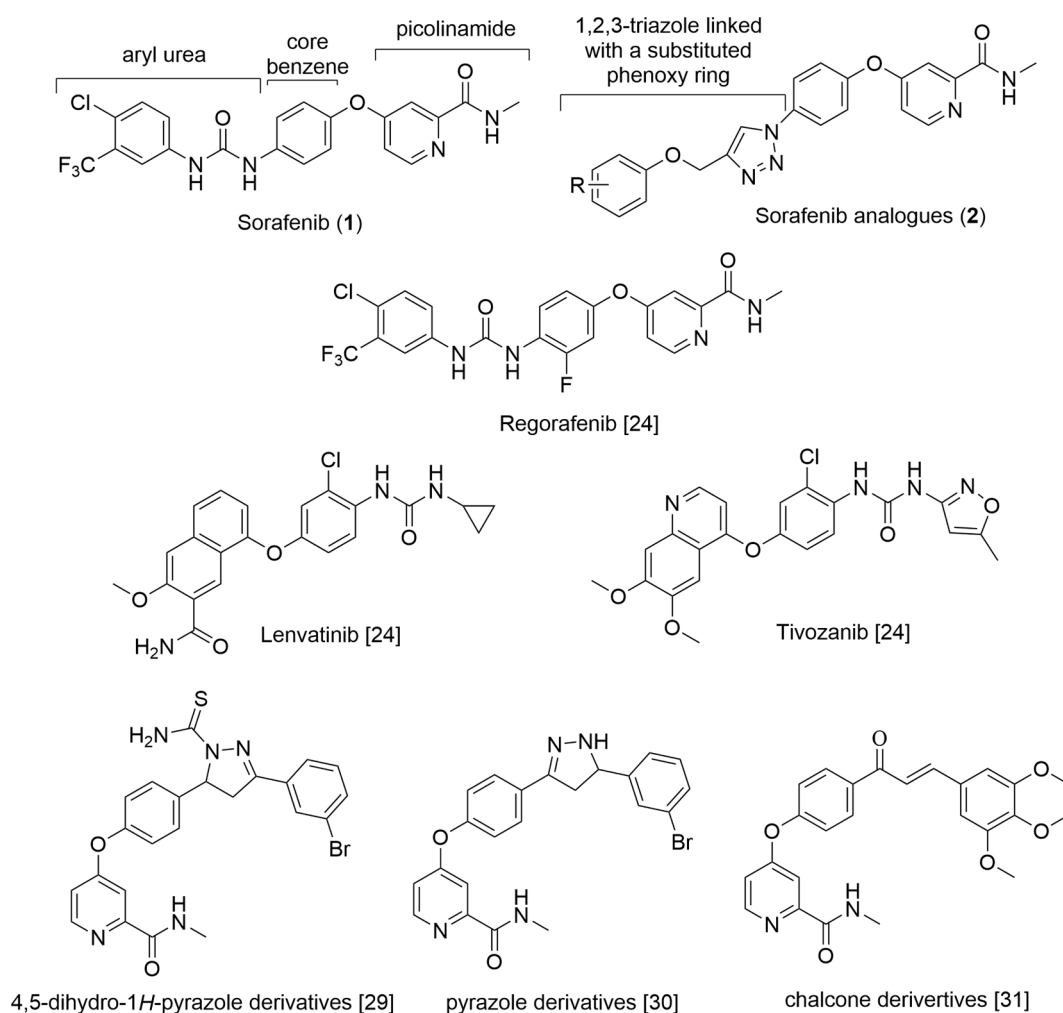


Fig. 1. The chemical structures of Sorafenib (1), 1,2,3-triazole-containing Sorafenib analogues (2), Regorafenib, Lenvatinib, Tivozanib and picolinamide derivatives.

compensation from other structural features. Instead of aryl urea of Sorafenib, 1,2,3-triazole linking with a substituted phenoxy ring could be a suitable counterpart (structure **2**, Fig. 1). The triazole heterocycle could provide hydrogen bonding, hydrophobic and π - π modes of binding to the targets, whereas the terminal substituted phenoxy tether could offer hydrophobic interaction with the lipophilic pocket. Additionally, the triazole structure has been proved to be metabolically stable [38] and this structure has been presented in a wide variety of bioactive compounds including analgesic, anti-bacterial, anti-fungal, anti-inflammatory, anti-malarial, anti-tubercular, anti-leishmanial, antiviral, anti-tumor agents [39–41].

Herein, we report the synthesis of the 1,2,3-triazole-containing Sorafenib analogues and their cytotoxicity towards human hepatocellular carcinoma (HCC) cell lines, HepG2 and Huh7, in order to study their structure–activity relationships (SARs). The safety profile of analogues was examined by testing with human embryonal lung fibroblast cell line, MRC-5, and the selectivity index (SI) was evaluated. Additionally, the inhibitory activity of the selected active analogue(s) was explained by molecular docking studies in B-RAF and VEGFR2 models and confirmed by cell migration and cell proliferation assays.

2. Results and discussion

2.1. Chemistry

The designed triazole-containing Sorafenib analogues **2a-2g** from our preliminary work [42] and additional analogues **2h-2ac** were synthesized successfully via Huisgen 1,3-dipolar cycloaddition followed by nucleophilic aromatic substitution, whereas the preparation of analogue **2ad** was accomplished via reduction as illustrated in Scheme 1.

Initially, various phenols **3** were *O*-propargylated using propargyl bromide (**4**) under basic conditions to give the corresponding alkynes **5** with moderate to excellent yields. Subsequently, the 1,2,3-triazole rings were constructed using Huisgen 1,3-dipolar cycloaddition between the obtained alkynes **5** and 4-azidophenol (**6**), which was prepared via diazotization using the conditions described previously [43], leading to the formation of the triazoles **7** in the yields of 25–96% [44]. After coupling with 4-chloropicolinamide (**8**) [45] in the presence of *tert*-butoxide and potassium carbonate, the triazole-containing phenols **7**

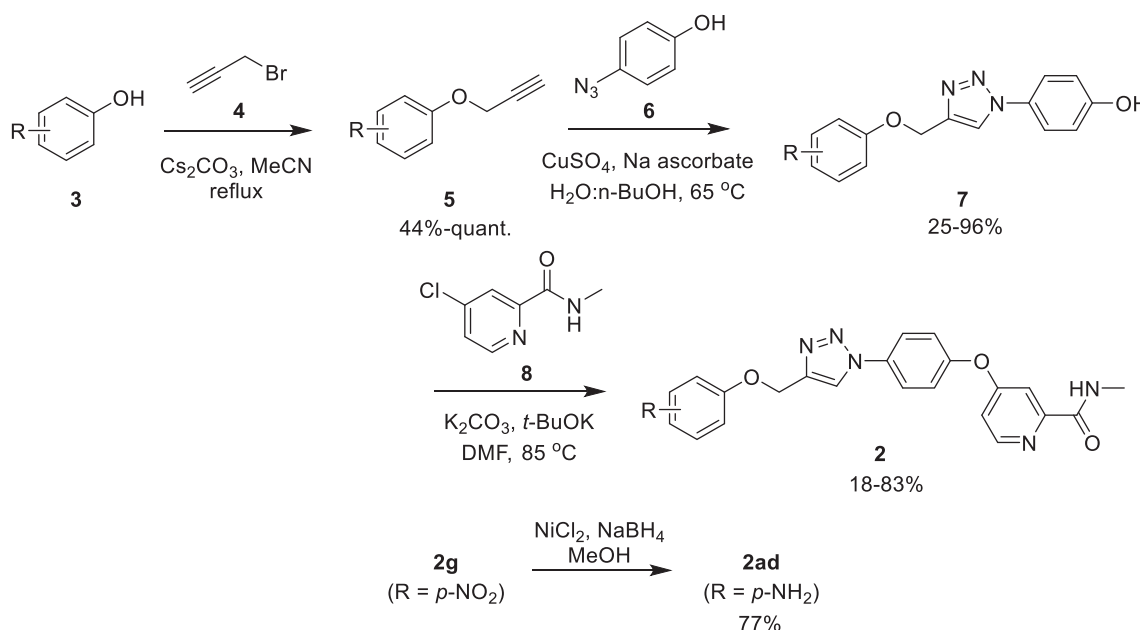
were transformed to the target Sorafenib analogues **2a-2ac** in the yields of 18–83%. In the synthesis of **2aa** (R = *p*-OH), 4-((*tert*-butyldimethylsilyloxy)phenol (**3aa**; R = *p*-OTBS) was used as a starting material. The corresponding alkyne **5aa** (R = *p*-OTBS) and phenol **7aa** (R = *p*-OTBS) were obtained using the conditions described above. The final target **2aa** (R = *p*-OH) were obtained after coupling **7aa** (R = *p*-OTBS) and picolinamide **8** in moderate yield (31%). While, the preparation of the analogue **2ad** (R = *p*-NH₂) was accomplished by Ni-catalyzed reduction of the target compound **2g** (R = *p*-NO₂) in a good yield (77%) (Scheme 1) [46]. Structures of the synthetic Sorafenib analogues **2a-2ad** were confirmed by NMR and HRMS techniques. Typically, ¹H NMR spectra showed a singlet peak of OCH₂ and H on the triazole at δ 5.2 to 5.4 and 8.1 to 9.9 ppm, respectively. Two doublet peaks at δ 6.5 to 8.5 ppm with $J \approx 9$ Hz confirmed the *p*-substituted benzene. ¹⁹F atom(s) of F and CF₃ were observed by ¹⁹F NMR spectra at δ –165 to –110 and –65 to –60 ppm, respectively. The couplings of ¹³C and ¹⁹F were appeared on the ¹³C NMR spectra with ¹ J = 235–270 Hz, ² J = 10–40 Hz and ³ J = 4–20 Hz. The NMR spectra of picolinamide part were consistent with those reported in the literature [45].

2.2. Biological evaluation

The biological activities towards HepG2 and Huh7 of the synthetic triazole-containing analogues **2h-2ad** were evaluated in *in vitro* model using MTT assay [47,48] compared to **2a-2g** [42]. These two HCC cell lines are distinguishable by their origins and gene profiles leading to different expressions and responses to the drug treatments [49,50]. Furthermore, their cytotoxicity towards MRC-5 of all target compounds **2a-2ad** was also examined [51]. The results were reported as half-maximal inhibitory concentration (IC₅₀) values in micromolar range (μ M) and selectivity index (SI) of each compounds was calculated for expression of their safety profile.

2.2.1. Cytotoxicity towards HepG2 and Huh7

Several substituents (H, F, NO₂, CF₃ and *t*-Bu) were introduced to the phenoxy ring linked with the triazole at *o*-, *m*- and *p*-position in order to investigate positions and types of substituents impacting the inhibition of the HCC cell lines. Their inhibitory activities were showed in Table 1. In the first series of compounds **2a-2m**, it was found that all the active



Scheme 1. The synthetic pathways to the triazole-containing Sorafenib analogues **2a-2ac** starting from various phenols **3a-3ac** and analogue **2ad** from the target compound **2g**.

Table 1

In vitro inhibitory activities towards HCC cell lines, HepG2 and Huh7, and human embryonal lung fibroblast cell line, MRC-5, of the synthetic Sorafenib analogues **2a-2ad**, compared to Sorafenib. The half-maximal inhibitory concentration (IC₅₀) in micromolar (μM) scale and the selectivity index (SI) were reported.

Compound	R	IC ₅₀ (μM)			SI	
		HepG2	Huh7	MRC-5	HepG2	Huh7
2a	H	>100	>100	>100	–	–
2b	<i>o</i> -F	>100	>100	>100	–	–
2c	<i>m</i> -F	>100	>100	>100	–	–
2d	<i>p</i> -F	>100	64.4 ± 5.5	>100	–	>1.55
2e	<i>o</i> -NO ₂	72.0 ± 5.5	52.5 ± 0.8	>100	>1.39	>1.90
2f	<i>m</i> -NO ₂	>100	>100	>100	–	–
2g	<i>p</i> -NO ₂	>100	21.1 ± 5.9	94.4 ± 0.81	–	4.48
2h	<i>o</i> -CF ₃	>100	>100	>100	–	–
2i	<i>m</i> -CF ₃	>100	>100	>100	–	–
2j	<i>p</i> -CF ₃	>100	50.9 ± 0.4	>100	–	>1.96
2k	<i>o</i> - <i>t</i> Bu	>100	>100	>100	–	–
2l	<i>m</i> - <i>t</i> Bu	61.6 ± 5.2	47.3 ± 1.1	16.5 ± 2.49	0.27	0.35
2m	<i>p</i> - <i>t</i> Bu	>100	5.67 ± 0.57	>100	–	>17.6
2n	2,3-F	>100	>100	>100	–	–
2o	2,4-F	>100	>100	>100	–	–
2p	2,5-F	>100	>100	>100	–	–
2q	2,6-F	>100	>100	>100	–	–
2r	3,4-F	>100	>100	>100	–	–
2s	3,5-F	>100	>100	>100	–	–
2t	3,5-CF ₃	>100	>100	>100	–	–
2u	3-CF ₃ , 4-Cl	>100	>100	68.7 ± 4.68	–	–
2v	<i>p</i> -Me	>100	>100	>100	–	–
2w	<i>p</i> -Et	>100	>100	>100	–	–
2x	<i>p</i> - <i>i</i> Pr	>100	>100	>100	–	–
2y	<i>p</i> -Cl	>100	>100	65.46 ± 0.99	–	–
2z	<i>p</i> -Br	>100	>100	>100	–	–
2aa	<i>p</i> -OH	84.0 ± 4.6	36.2 ± 4.4	>100	>1.19	>2.76
2ab	<i>p</i> -OMe	>100	>100	>100	–	–
2ac	<i>p</i> -NHAc	>100	>100	>100	–	–
2ad	<i>p</i> -NH ₂	>100	>100	>100	–	–
Sorafenib		3.87 ± 1.74	2.93 ± 0.65	19.7 ± 1.68	5.10	6.73

compounds **2d** (R = *p*-F), **2e** (R = *o*-NO₂), **2g** (R = *p*-NO₂), **2j** (R = *p*-CF₃), **2l** (R = *m*-*t*Bu) and **2m** (R = *p*-*t*Bu) inhibited Huh7 (IC₅₀ < 100 μM) with significantly higher activity than HepG2. Obviously, analogues with *p*-substitution (**2d** (R = *p*-F), **2g** (R = *p*-NO₂), **2j** (R = *p*-CF₃) and **2m** (R = *p*-*t*Bu)) exhibited superior IC₅₀ against Huh7 compared to the corresponding *o*- and *m*-substitution. Only compounds **2e** (R = *o*-NO₂) and **2l** (R = *m*-*t*Bu) showed mild activity against both HepG2 and Huh7 with IC₅₀ lower than 100 μM. We next investigated the disubstituted analogues **2n-2u**, consisting of difluoro-, di(trifluoromethyl)- and 3-trifluoromethyl-4-chlorophenoxy (analogous to Sorafenib). It was found that all these disubstituted analogues were inactive (IC₅₀ > 100 μM) towards both HCC cell lines. A plan for syntheses of other disubstituted analogues was therefore terminated.

Based on the first series of compounds **2a-2m**, it was evident that *p*-substituted analogues had a potential for further improvement. Therefore, a variety of substituents were attached to the phenoxy ring at *p*-position consisting of nonpolar alkyl, halogen, hydroxy, methoxy, amino, *N*-acetamido groups as shown as **2v-2ad** in Table 1. However, the IC₅₀ values of most compounds in this set were higher than 100 μM, except the hydroxy-substituted analogue **2aa** (R = *p*-OH) that showed moderate inhibitory activities with IC₅₀ = 84.0 ± 4.6 and 36.2 ± 4.4 μM towards HepG2 and Huh7, respectively. In summary, the synthesized

analogues showed moderate to no activity against HepG2 with the best IC₅₀ = 61.6 ± 5.2 μM. For Huh7, several compounds showed good inhibitory activity, of which the *p*-analogue **2m** (R = *p*-*t*Bu) exhibited the best inhibitory activity towards Huh7 with IC₅₀ = 5.67 ± 0.57 μM, followed by the *p*-analogue **2g** (R = *p*-NO₂) with IC₅₀ = 21.1 ± 5.9 μM.

It should be noted that activated extracellular signal-regulated kinase (phospho-ERK) is a clinical response biomarker to drug and combinatorial treatment in HCC liver cancers [52]. Inhibition of Huh7, which expresses high level of phospho-ERK, indicated that the agent **2m** could potentially suppress types of HCC that activated the phospho-ERK level. Furthermore, with the possible different molecular inhibition pathway to the mitogen-activated extracellular signal-regulated kinase (MEK) inhibitor drug, compound **2m** may possibly be used in the combination for synergistic effect in the HCC treatment.

2.2.2. Cytotoxicity towards MRC-5 and selectivity index (SI)

Regarding compounds' toxicity, the cytotoxicity against MRC-5 of all the synthesized compounds was investigated using procedure described previously [51]. The results showed that most of compounds were non-cytotoxic at 100 μM as shown in Table 1. Only **2l** (R = *m*-*t*Bu) possessed IC₅₀ = 16.5 ± 2.49 μM for MRC-5, which was more toxic than Sorafenib (IC₅₀ = 19.7 ± 1.68 μM). The best anti-Huh7 agents **2g** (R = *p*-NO₂) and **2m** (R = *p*-*t*Bu) exhibited the cytotoxicity towards MRC-5 at IC₅₀ = 94.4 ± 0.81 μM and > 100 μM, respectively, which were much safer than Sorafenib. More importantly, these two compounds (**2g** and **2m**) have highly selective cytotoxic activity towards Huh7 with SI = 4.48 and > 17.6, respectively. It is also worth mentioned that compound **2m** (R = *p*-*t*Bu) showed much higher selectivity than Sorafenib (SI = 6.73) for Huh7. With the promising inhibitory activity and safety profile, **2m** (R = *p*-*t*Bu) and **2g** (R = *p*-NO₂) were selected for further molecular docking studies.

2.3. Molecular docking studies with B-RAF and VEGFR2

To gain better understanding of intermolecular interactions between our compounds and the cavity of important targets B-RAF and VEGFR2, molecular docking was performed using iGEMDOCK v2.1 software [53]. Our first two compounds with the lowest IC₅₀ (**2m** and **2g**) were docked into the active site of B-RAF co-crystallized with Sorafenib (PDB ID:1uwH) and VEGFR2 co-crystallized with Sorafenib (PDB ID:4asD). Sorafenib was also redocked into the B-RAF and VEGFR2, and its binding energies were compared with those of our compounds.

As illustrated in Figure S75 (supporting information), the redocked Sorafenib had similar binding position to co-crystallized Sorafenib in B-RAF and VEGFR2. For B-RAF, Fig. 2a-2b demonstrated that both **2m** and **2g** interacted efficiently with the active site of the B-RAF near the Sorafenib binding position. The *p*-*tert*-butyl phenoxy ring of **2m** bound at the same position as that of trifluoromethyl phenyl ring of Sorafenib. The bulky substitution group on the phenoxy ring of **2m** were at *p*-position, whereas trifluoromethyl group on the phenoxy ring of Sorafenib was at 3-position. As a consequence, the rest of the molecule of **2m** lay in different direction, locating between αC-helix and P-loop of the B-RAF. Additionally, pyridine of **2m** bound very close to oxygen of Met483 with 2.76 Å (Fig. 2c). For compound **2g**, the binding positions of pyridyl ring and 1,2,3-triazole ring of **2g** in B-RAF were similar to those of central ring and trifluoromethyl phenyl ring of co-crystallized Sorafenib, respectively, while its phenoxy ring was located near αC-helix of B-RAF. In addition, the molecular docking in Fig. 2d revealed that nitro group of **2g** was adjacent to the side chain of Ala496 with 2.52 Å. The binding energies for **2m** and **2g** were –113.79 and –110.70 kcal/mol, respectively, which were slightly higher than that of redocked Sorafenib (–117.29 kcal/mol) (Table 2).

As can be seen in Fig. 3a-3b, **2m** and **2g** fit well the active site of VEGFR2 with more or less the same binding position to that of co-crystallized Sorafenib and their binding energies were –115.33 and –111.40 kcal/mol for **2m** and **2g**, respectively, which were higher than that of Sorafenib (–130.58 kcal/mol) (Table 2). Fig. 3c-3d revealed that

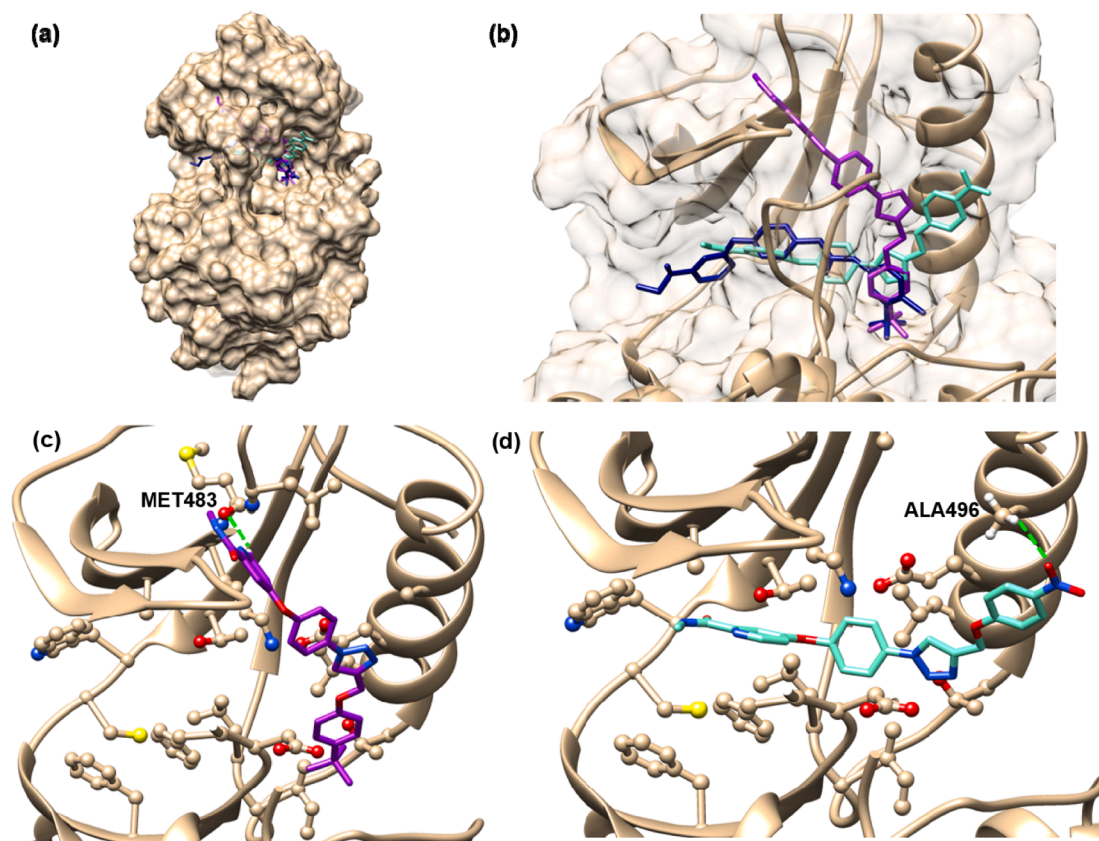


Fig. 2. Comparison of binding positions of **2m** (purple), **2g** (light blue) and the co-crystallized Sorafenib (deep blue) in the cavity of B-RAF (PDB ID: 1uwf), (b) the comparison of **2m** (purple), **2g** (light blue) and the co-crystallized Sorafenib (deep blue) (a,b), and the interacting residues with **2m** (c) and **2g** (d) in the binding site of B-RAF. (For interpretation of the references to colour in this figure legend, the reader is referred to the web version of this article.)

Table 2

Binding energies, amino acid residues and bond lengths of **2m**, **2g** and the redocked Sorafenib in binding site of B-RAF and VEGFR2.

Compound	Binding energy (kcal/mol)	Amino acid residue	Bond length (Å)
<i>B-RAF</i>			
2m	-113.79	Met483:O	2.76
2g	-110.70	Ala496:H	2.52
Sorafenib (1)	-117.29	Glu500:O, Asp593:H	2.65, 2.10
<i>VEGFR2</i>			
2m	-115.33	Asp1046:H, Lys920:O, Cys919:O, Glu885:O	2.50, 2.07, 1.97, 2.44
2g	-111.40	Asp1046:H, His1026:O, Glu885:O	2.47, 2.80, 2.54
Sorafenib (1)	-130.58	Cys1045:H, Cys919:O, Glu917:O, Glu885:O	2.85, 2.23, 2.55, 2.67

both **2m** and **2g** formed hydrogen bonding with Asp1046 and Glu885. Additionally, nitro group of **2g** interacted with the side chain of His1026 while methyl amide of **2m** bound very close to oxygen of Cys919 and Lys920. Sorafenib also bound with Cys919 and Glu885 in the active site of VEGFR2.

It can be noted that, comparing between **2g** and **2m**, compound **2m** with lower IC₅₀ value displayed lower binding energies than those of **2g**, thus the molecular docking results were in agreement with the IC₅₀ values.

2.4. Biochemistry

2.4.1. Inhibitory activity towards B-RAF

In order to gain information related to its anti-cancer activity, compound **2m** was selected to investigate inhibitory activity towards B-RAF *in vitro* compared to Sorafenib. As a result, **2m** exhibited moderate activity towards B-RAF, whereas Sorafenib inhibited B-RAF efficiently as illustrated in Fig. 4. Based on the anti-Huh7 effect, and the docking study in B-RAF model indicating that laying position of **2m** was near but differed from that of Sorafenib (Fig. 2b) and **2m** had higher binding energy, it could be implied that the anti-Huh7 activity of **2m** might not strictly be influenced by the inhibition of B-RAF. Potentially, **2m** might inhibit other kinases in the same pathway, for example VEGFR2, in which **2m** fit very well at the Sorafenib position (Fig. 3b), and/or, possibly, involve in different mechanism of action or pathway from the parent Sorafenib [54].

2.4.2. Wound healing assay

To investigate the effect of the candidate compound **2m**, which had the lowest IC₅₀ with the highest SI among the series and comparable binding energy to Sorafenib, on the migration of HCC cells, wound healing assay was performed [55]. Huh7 cells were exposed to the concentration of 3 μM of Sorafenib and 3, 6 and 12 μM of **2m** for 0, 24 and 48 h. The results showed the suppression of cell migration of Huh7 with time- and dose-dependent manner as represented in Fig. 5. Wound healing percentage of each compound and each concentration are unidentical. Increasing of dose declined healing percentage and time extension developed the recovery. Sorafenib at the concentration of 3 μM exhibited cell repair inhibition almost ten folds compared to control, while **2m** at the concentration of 12 μM suppressed wound repair only two folds (see Figure S76, supporting information). These results

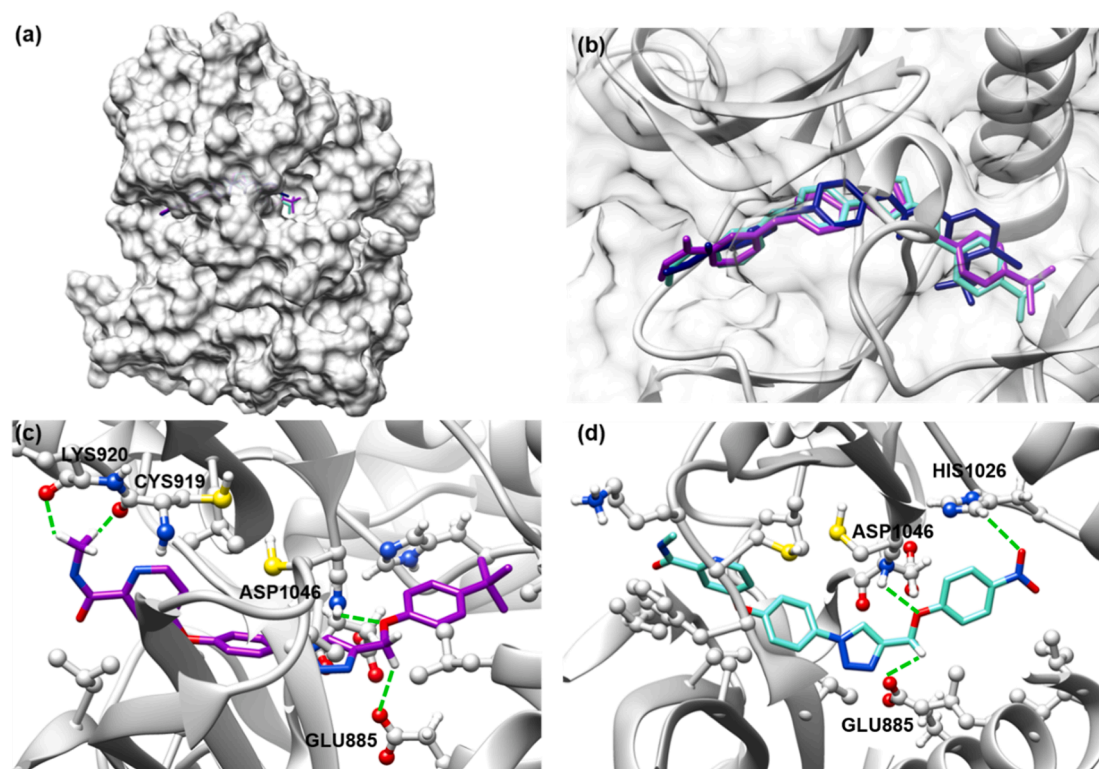


Fig. 3. Comparison of binding positions of **2m** (purple), **2g** (light blue) and the co-crystallized Sorafenib (deep blue) in the cavity of VEGFR2 (PDB ID: 4asd), (b) the comparison of **2m** (purple), **2g** (light blue) and the co-crystallized Sorafenib (deep blue) (a,b), and the interacting residues with **2m** (c) and **2g** (d) in the binding site of VEGFR2. (For interpretation of the references to colour in this figure legend, the reader is referred to the web version of this article.)

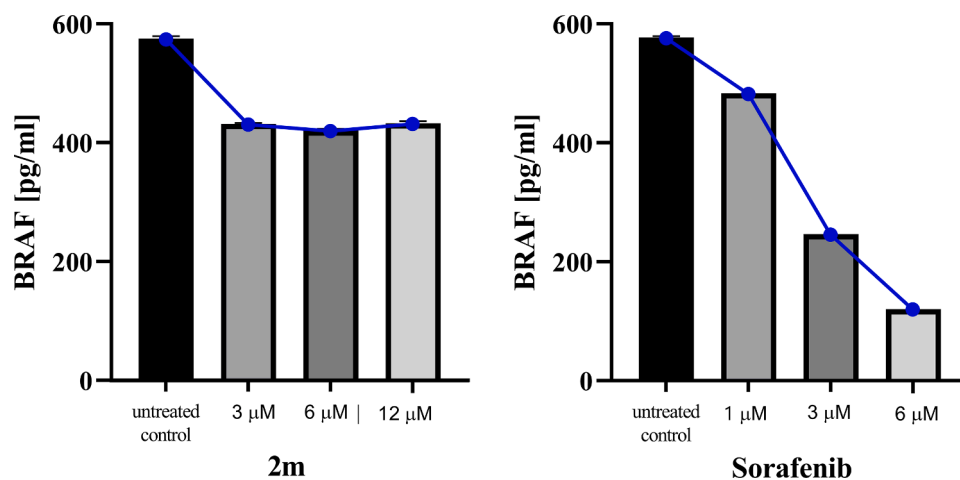


Fig. 4. Inhibitory activity towards B-RAF of **2m** (left) and Sorafenib (right).

suggested that **2m** can inhibit the cell migration of Huh7 cell compared to control; however, it was less potent inhibitor of cell migration than Sorafenib.

2.4.3. Anti-proliferative activity

To demonstrate the effect of **2m** on DNA synthesis in Huh7 cells, BrdU cell proliferation was performed to identify the anti-cell proliferative activity [56]. As shown in Fig. 6, at 24 h, BrdU incorporation was reduced in Sorafenib and **2m** treated cells when compared to the untreated cells, suggesting DNA synthesis was inhibited. Similarly, at 48 h, DNA synthesis was also inhibited by Sorafenib and **2m** at 6 and 12 μM. The time-dependent pattern of **2m** was rather constant over time, implying that **2m** inhibited cell proliferation of Huh7 in a dose-

dependent manner. However, Sorafenib showed superior anti-cell proliferative properties significantly to the Sorafenib analogue **2m**.

3. Conclusion

New triazole-containing Sorafenib analogues were synthesized successfully with high yields via Huisgen 1,3-dipolar cycloaddition, nucleophilic substitution and functional group transformation. The triazole-containing analogues with bulky substituent at *p*-position on the terminal phenoxy ring seems to be the necessary structural feature for selective Huh7 inhibition with high safety profile. Among the compounds in this series, analogue **2m** expressed the best inhibitory activity against Huh7, but it was inactive for HepG2. The different responses to the

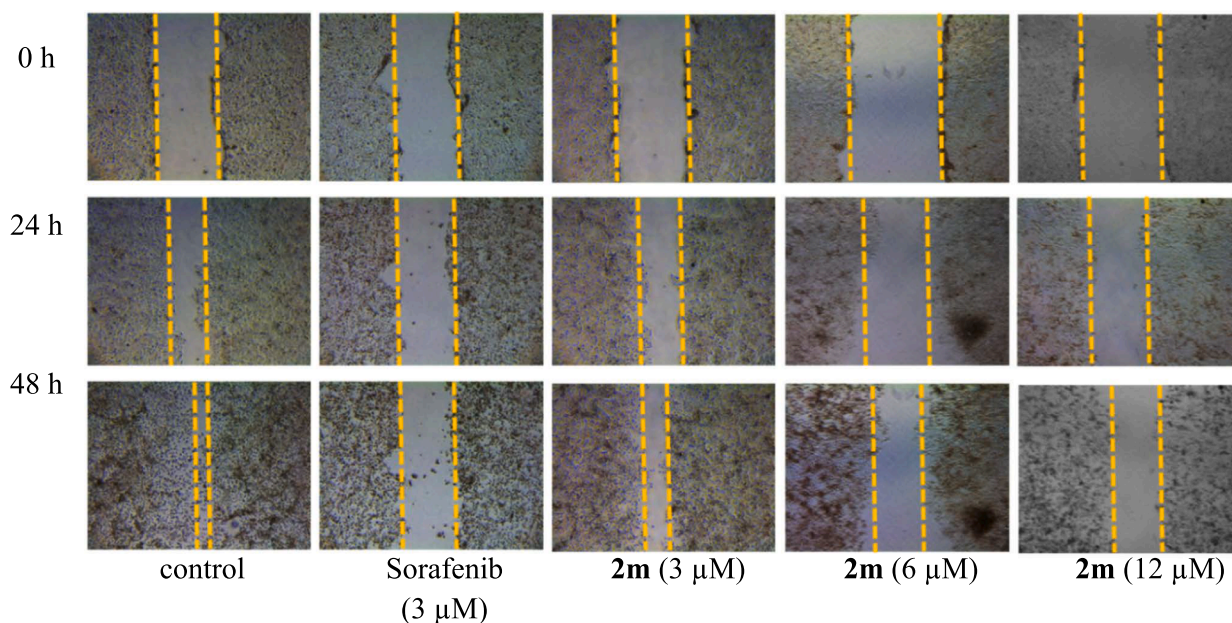


Fig. 5. Wound healing assay in Huh7 of compound **2m** at the concentration of 3, 6 and 12 μM for 0, 24 and 48 h, compared to control and Sorafenib at the concentration of 3 μM .

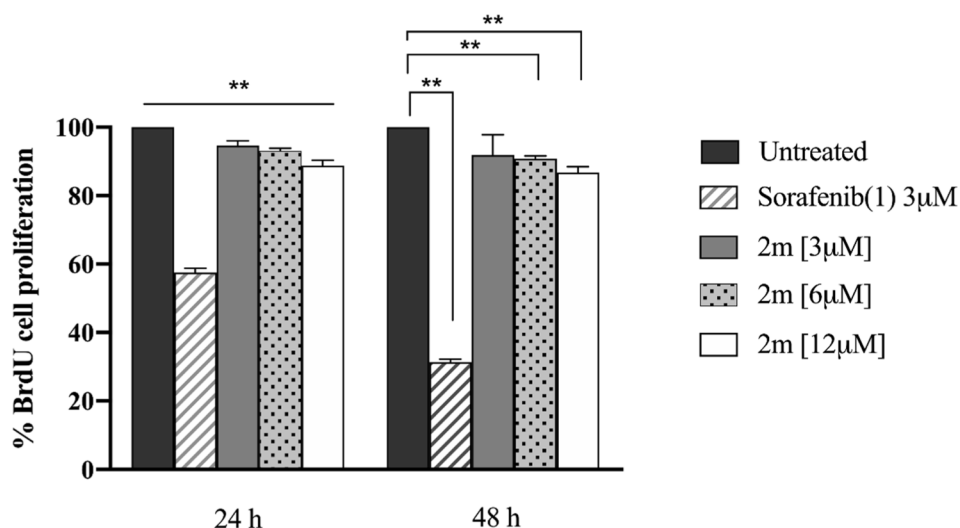


Fig. 6. Cell proliferation activity assay in Huh7 of **2m** at the concentration of 3, 6 and 12 μM for 24 and 48 h using BrdU cell proliferation kit, compared to Sorafenib at the concentration of 3 μM . Data are expressed as the percentage (Mean \pm SD), $n = 3$, $**P < 0.01$ compared with the untreated cells (control).

treatment might be due to different gene profiles. Although **2m** exhibited IC_{50} towards Huh7 ca. 2-fold less active than Sorafenib, the cytotoxicity against normal human lung fibroblast cell line, MRC-5, indicated that **2m** was obviously less toxic than Sorafenib. The SI for Huh7 of **2m** was at least 2.6-fold superior to that of Sorafenib. The molecular docking studies confirmed the efficient interaction of **2m** with B-RAF and VEGFR2, near and the same Sorafenib's binding site, respectively. In addition, the active analogue **2m** showed the inhibition of cell migration of Huh7 with time- and dose-dependent fashion and anti-cell proliferative activity with dose-dependent fashion. However, moderate inhibitory activity towards B-RAF of **2m** was evident that its anti-Huh7 activity might not directly relate to the inhibition of B-RAF. The mechanism of action should be further investigated. The current study evidently identified **2m** as a promising candidate with high safety profile for further development of anti-HCC agents. Its Huh7 inhibitory property emphasized the potentiality of using **2m** in treatment of the HCC with high phospho-ERK level as well as using **2m** as the drug

combination with other inhibitors in HCC clinical therapy.

4. Experimental part

4.1. Chemicals and materials

Chemicals and reagents used were purchased from Acros Organics, Sigma-Aldrich and Tokyo Chemical Industry (TCI). All reagents received were analytical grade and used without purification, unless stated otherwise. Deionized water was used in this work. Preparative chromatographic separations were performed on silica gel 63–200 μm purchased from Merck. All reactions were followed by TLC analysis using precoated silica gel 60 TLC sheets (Merck) with fluorescent indicator (254 nm) and visualized with a UV lamp (254 and 365 nm).

4.2. Instruments

^1H , ^{13}C and ^{19}F NMR spectra were recorded on a Bruker AVANCE III HD in Fourier transform mode at the field strength specified on a 300 MHz spectrometer. DEPT and 2D NMR spectra including COSY, HMQC and HMBC of some compounds were collected for clarifying the structures. Spectra were obtained in CDCl_3 and $\text{DMSO}-d_6$ solutions using 5 mm diameter tubes, and chemical shifts in ppm (part per million) are quoted relative to either the internal standards, TMS (δ_{H} 0.00) or CF_3COOH (δ_{F} -76.55) or the residual signals of either CDCl_3 (δ_{H} 7.26, or δ_{C} 77.22) or $\text{DMSO}-d_6$ (δ_{H} 2.50, or δ_{C} 39.51). Data are reported as follows: chemical shifts, multiplicity, coupling constant. Multiplicities in the ^1H and ^{19}F NMR spectra are described as: s = singlet, d = doublet, t = triplet, q = quartet, m = multiplet, br = broad; coupling constants (J) are reported in Hz. High-resolution mass spectra (HRMS) are recorded using a Bruker Daltonics MicroTOF mass spectrometer with ESI + mode and reported with ion mass/charge (m/z) ratios as values in atomic mass units.

4.3. Chemistry

4.3.1. Preparation of alkynes 5

General procedure A: Preparation of alkyne derivatives 5a-5ac [42]

At room temperature, neat propargyl bromide or a solution of 80% propargyl bromide (**4**) in THF (1.0–1.5 eq.) was added dropwise to a stirred suspension of phenol derivatives (1.0 eq.) in CH_3CN and Cs_2CO_3 (1.0–2.0 eq.). The resulting mixture was stirred at room temperature overnight or heated to reflux for 2–24 h. The resulting mixture was diluted with water and extracted with EtOAc. The organic phases were combined and concentrated under reduced pressure to provide crude propargyl derivatives. The residue was purified by silica gel column chromatography to furnish the desired products **5a-5ac**.

(pro-2-yn-1-yloxy)benzene (**5a**) [42]

Purification by silica gel column chromatography using *n*-hexane as eluent gave a pale pink liquid with 44% yield. ^1H NMR (300 MHz, CDCl_3) δ 2.52 (t, $J = 2.4$ Hz, 1H), 4.69 (d, $J = 2.4$ Hz, 2H), 6.99 (m, 3H), 7.31 (m, 2H) ppm.; ^{13}C NMR (75 MHz, CDCl_3) δ 30.9, 55.7, 76.7, 113.8, 121.9, 129.5, 157.6 ppm.

1-fluoro-2-(pro-2-yn-1-yloxy)benzene (**5b**) [42]

Purification by silica gel column chromatography using *n*-hexane as eluent gave colorless oil with 92% yield. ^1H NMR (300 MHz, $\text{DMSO}-d_6$) δ 3.61 (t, $J = 2.3$ Hz, 1H), 4.88 (d, $J = 2.4$ Hz, 2H), 6.98 (m, 3H), 7.19 (m, 3H) ppm.; ^{13}C NMR (75 MHz, $\text{DMSO}-d_6$) δ 56.4, 78.7, 78.8, 115.7, 116.2 (d, $^2J_{\text{FC}} = 17.3$ Hz), 121.9 (d, $^3J_{\text{FC}} = 6.8$ Hz), 124.7 (d, $^3J_{\text{FC}} = 3.8$ Hz), 145.0 (d, $^2J_{\text{FC}} = 9.8$ Hz), 151.9 (d, $^1J_{\text{FC}} = 242.3$ Hz) ppm.; ^{19}F NMR (282 MHz, $\text{DMSO}-d_6$) δ -136.4 (s, 1F) ppm.

1-fluoro-3-(pro-2-yn-1-yloxy)benzene (**5c**) [42]

Purification by silica gel column chromatography using *n*-hexane as eluent gave colorless liquid with 97% yield. ^1H NMR (300 MHz, CDCl_3) δ 2.53 (t, $J = 2.3$ Hz, 1H), 4.67 (d, $J = 2.3$ Hz, 2H), 6.67 (m, 3H), 7.24 (m, 1H) ppm.; ^{13}C NMR (75 MHz, CDCl_3) δ 56.0, 75.9, 78.1, 102.8 (d, $^2J_{\text{FC}} = 24.8$ Hz), 108.4 (d, $^2J_{\text{FC}} = 21.8$ Hz), 110.6 (d, $^4J_{\text{FC}} = 3.4$ Hz), 130.3 (d, $^3J_{\text{FC}} = 9.8$ Hz), 158.8 (d, $^3J_{\text{FC}} = 3.8$ Hz), 163.5 (d, $^1J_{\text{FC}} = 243.8$ Hz) ppm.; ^{19}F NMR (282 MHz, CDCl_3) δ -112.2 (s, 1F) ppm.

1-fluoro-4-(pro-2-yn-1-yloxy)benzene (**5d**) [42]

Purification by silica gel column chromatography using *n*-hexane as eluent gave colorless liquid with 76% yield. ^1H NMR (300 MHz, CDCl_3) δ 2.51 (t, $J = 2.4$ Hz, 1H), 4.64 (d, $J = 2.4$ Hz, 2H), 6.95 (m, 4H) ppm.; ^{13}C NMR (75 MHz, CDCl_3) δ 56.5, 75.7, 78.5, 115.9 (d, $^2J_{\text{FC}} = 23.2$ Hz), 116.2 (d, $^3J_{\text{FC}} = 8.0$ Hz), 153.7 (d, $^4J_{\text{FC}} = 2.2$ Hz), 157.8 (d, $^1J_{\text{FC}} = 237.7$ Hz) ppm.; ^{19}F NMR (282 MHz, $\text{DMSO}-d_6$) δ -124.8 (s, 1F) ppm.

1-nitro-2-(prop-2-yn-1-yloxy)benzene (**5e**) [42]

Purification by silica gel column chromatography using 15% EtOAc: *n*-hexane as eluent gave yellow solid with quantitative yield. ^1H NMR (300 MHz, CDCl_3) δ 2.59 (t, $J = 3.0$ Hz, 1H), 4.81 (d, $J = 3.0$ Hz, 2H), 7.1

(dd, $J = 6.0$, 3.0 Hz, 2H), 8.24 (dd, $J = 6.0$, 3.0 Hz, 2H) ppm.; ^{13}C NMR (75 MHz, CDCl_3) δ 57.2, 77.1, 77.2, 115.5, 121.4, 125.7, 134.0, 140.4, 150.8 ppm.

1-nitro-3-(prop-2-yn-1-yloxy)benzene (**5f**) [42]

Purification by silica gel column chromatography using 15% EtOAc: *n*-hexane as eluent gave yellow solid with 97% yield. ^1H NMR (300 MHz, CDCl_3) 2.59 (t, $J = 2.4$ Hz, 1H), 4.79 (d, $J = 2.4$ Hz, 2H), 7.31 (ddd, $J = 8.3$, 2.6, 0.9 Hz, 1H), 7.47 (t, $J = 8.2$ Hz, 1H), 7.83 (t, $J = 2.3$ Hz, 1H), 7.88 (ddd, $J = 8.2$, 2.1, 0.9 Hz, 1H) ppm.; ^{13}C NMR (75 MHz, CDCl_3) δ 56.3, 76.7, 77.3, 109.6, 116.6, 121.9, 130.1, 149.1, 157.9 ppm.

1-nitro-4-(prop-2-yn-1-yloxy)benzene (**5g**) [42]

Purification by silica gel column chromatography using 15% EtOAc: *n*-hexane as eluent gave yellow solid with quantitative yield. ^1H NMR (300 MHz, CDCl_3) δ 2.59 (t, $J = 3.0$ Hz, 1H), 4.81 (d, $J = 3.0$ Hz, 2H), 7.1 (dd, $J = 6.0$, 3.0 Hz, 2H), 8.24 (dd, $J = 6.0$, 3.0 Hz, 2H) ppm.; ^{13}C NMR (75 MHz, $\text{DMSO}-d_6$) δ 56.3, 78.2, 79.1, 115.0, 125.8, 141.4, 162.3 ppm.

1-(prop-2-yn-1-yloxy)-2-(trifluoromethyl)benzene (**5h**) [57]

Purification by silica gel column chromatography using *n*-hexane as eluent gave colorless oil with 98% yield. ^1H NMR (300 MHz, CDCl_3) δ 2.53 (t, $J = 2.3$ Hz, 1H), 4.79 (d, $J = 2.3$ Hz, 2H), 7.06 (t, $J = 7.6$ Hz, 1H), 7.16 (d, $J = 8.4$ Hz, 1H), 7.51 (t, $J = 7.6$ Hz, 1H), 7.59 (d, $J = 7.6$ Hz, 1H) ppm.; ^{13}C NMR (75 MHz, CDCl_3) δ 56.4, 76.2, 77.8, 113.6, 123.5 (q, $^1J_{\text{FC}} = 270.7$ Hz), 119.5 (q, $^2J_{\text{FC}} = 30.8$ Hz), 121.0, 127.3 (q, $^3J_{\text{FC}} = 5.3$ Hz), 133.1, 155.4 (q, $^4J_{\text{FC}} = 1.6$ Hz) ppm.; ^{19}F NMR (282 MHz, CDCl_3) δ -62.9 (s, 3F) ppm.

1-(prop-2-yn-1-yloxy)-3-(trifluoromethyl)benzene (**5i**) [57]

Purification by silica gel column chromatography using *n*-hexane as eluent gave colorless oil with 85% yield. ^1H NMR (300 MHz, CDCl_3) δ 3.61 (t, $J = 2.4$ Hz, 1H), 4.92 (d, $J = 2.4$ Hz, 2H), 7.32 (m, 3H), 7.55 (m, 1H) ppm.; ^{13}C NMR (75 MHz, CDCl_3) δ 55.9, 78.7, 78.7, 111.48 (q, $^3J_{\text{FC}} = 3.8$ Hz), 117.9 (q, $^3J_{\text{FC}} = 3.9$ Hz), 119.3, 124.0 (q, $^1J_{\text{FC}} = 270.7$ Hz), 130.4 (q, $^2J_{\text{FC}} = 31.6$ Hz), 130.7, 157.5 ppm.; ^{19}F NMR (282 MHz, CDCl_3) δ -62.9 (s, 3F) ppm.

1-(prop-2-yn-1-yloxy)-4-(trifluoromethyl)benzene (**5j**) [58]

Purification by silica gel column chromatography using *n*-hexane as eluent gave pale-yellow oil with quantitative yield. ^1H NMR (300 MHz, $\text{DMSO}-d_6$) δ 3.62 (t, $J = 2.3$ Hz, 1H), 4.91 (d, $J = 2.3$ Hz, 2H), 7.17 (d, $J = 8.8$ Hz, 2H), 7.66 (d, $J = 8.8$ Hz, 2H) ppm.; ^{13}C NMR (75 MHz, $\text{DMSO}-d_6$) δ 55.8, 78.6, 78.7, 115.3, 121.9 (q, $^2J_{\text{FC}} = 31.9$ Hz), 124.5 (q, $^1J_{\text{FC}} = 269.4$ Hz), 126.9 (q, $^3J_{\text{FC}} = 3.8$ Hz), 160.0 ppm.; ^{19}F NMR (282 MHz, $\text{DMSO}-d_6$) δ -61.5 (s, 3F) ppm.

1-(tert-butyl)-2-(prop-2-yn-1-yloxy)benzene (**5k**) [57]

Purification by silica gel column chromatography using *n*-hexane as eluent gave colorless oil with quantitative yield. ^1H NMR (300 MHz, CDCl_3) δ 1.39 (s, 9H), 2.47 (t, $J = 2.4$ Hz, 1H), 4.71 (d, $J = 2.4$ Hz, 2H), 6.93 (m, 2H), 7.18 (ddd, $J = 8.2$, 7.6, 1.7 Hz, 1H), 7.30 (dd, $J = 7.6$, 1.7 Hz, 1H) ppm.; ^{13}C NMR (75 MHz, CDCl_3) δ 29.9, 34.8, 55.5, 75.0, 78.9, 112.7, 121.2, 121.8, 126.9, 138.7, 156.5 ppm.

1-(tert-butyl)-3-(prop-2-yn-1-yloxy)benzene (**5l**) [57]

Purification by silica gel column chromatography using *n*-hexane as eluent gave colorless oil with 96% yield. ^1H NMR (300 MHz, CDCl_3) δ 1.31 (s, 9H), 2.51 (t, $J = 2.4$ Hz, 1H), 4.68 (d, $J = 2.4$ Hz, 2H), 6.79 (dd, $J = 7.9$, 2.5 Hz, 1H), 7.03 (m, 1H), 7.24 (m, 1H) ppm.; ^{13}C NMR (75 MHz, CDCl_3) δ 31.7, 34.8, 55.7, 75.4, 78.8, 111.0, 113.0, 118.7, 128.9, 153.1, 157.4 ppm.

1-(tert-butyl)-4-(prop-2-yn-1-yloxy)benzene (**5m**) [59]

Purification by silica gel column chromatography using *n*-hexane as eluent gave yellow oil with 85% yield. ^1H NMR (300 MHz, CDCl_3) δ 1.28 (s, 9H), 2.45 (t, $J = 2.4$ Hz, 1H), 4.61 (d, $J = 2.4$ Hz, 2H), 6.89 (d, $J = 8.7$ Hz, 2H), 7.29 (d, $J = 8.7$ Hz, 2H) ppm.; ^{13}C NMR (75 MHz, CDCl_3) δ 31.5, 34.0, 55.7, 75.3, 78.9, 114.3, 126.2, 144.1, 155.3 ppm.

1,2-difluoro-3-(prop-2-yn-1-yloxy)benzene (**5n**) [60]

Purification by silica gel column chromatography using *n*-hexane as eluent gave colorless oil with 77% yield. ^1H NMR (300 MHz, CDCl_3) δ 2.55 (t, $J = 2.4$ Hz, 1H), 4.78 (d, $J = 2.4$ Hz, 2H), 6.85 (m, 2H), 7.00 (m, 1H) ppm.; ^{13}C NMR (75 MHz, CDCl_3) δ 57.1, 76.5, 77.7, 110.3 (d, $^2J_{\text{FC}} =$

17.3 Hz), 111.0 (d, $^4J_{FC} = 3.0$ Hz), 123.1 (dd, $^3J_{FC}$, $^4J_{FC} = 9.0, 5.3$ Hz), 141.8 (dd, $^1J_{FC} = 246.7, 14.3$ Hz), 147.1 (dd, $^3J_{FC}$, $^4J_{FC} = 5.3, 3.0$ Hz), 151.5 (dd, $^1J_{FC}$, $^2J_{FC} = 246.0, 10.5$ Hz) ppm.; ^{19}F NMR (282 MHz, CDCl_3) δ -137.7 (s, 1F), -137.8 (s, 1F) ppm.

2,4-difluoro-1-(prop-2-yn-1-yloxy)benzene (5o) [61]

Purification by silica gel column chromatography using *n*-hexane as eluent gave colorless oil with 78% yield. ^1H NMR (300 MHz, CDCl_3) δ 2.54 (t, $J = 2.4$ Hz, 1H), 4.72 (d, $J = 2.4$ Hz, 2H), 6.79 (m, 2H), 7.08 (m, 1H) ppm.; ^{13}C NMR (75 MHz, CDCl_3) δ 58.2, 76.3, 78.0, 105.1 (dd, $^2J_{FC}$, $^2J_{FC} = 26.3, 21.8$ Hz), 110.5 (dd, $^2J_{FC}$, $^4J_{FC} = 22.5, 3.8$ Hz), 117.6 (dd, $^3J_{FC}$, $^3J_{FC} = 9.0, 2.3$ Hz), 114.9 (dd, $^2J_{FC}$, $^4J_{FC} = 10.5, 3.0$ Hz), 153.2 (dd, $^1J_{FC}$, $^3J_{FC} = 248.3, 12.0$ Hz), 157.4 (dd, $^1J_{FC}$, $^3J_{FC} = 241.5, 10.5$ Hz) ppm.; ^{19}F NMR (282 MHz, CDCl_3) δ -119.0 (d, $J_{FF} = 3.4$ Hz, 1F), -129.2 (d, $J_{FF} = 3.4$ Hz, 1F) ppm.

1,4-difluoro-2-(prop-2-yn-1-yloxy)benzene (5p) [62]

Purification by silica gel column chromatography using *n*-hexane as eluent gave colorless oil with 92% yield. ^1H NMR (300 MHz, CDCl_3) δ 2.58 (t, $J = 2.4$ Hz, 1H), 4.73 (d, $J = 2.4$ Hz, 2H), 6.63 (m, 1H), 6.85 (m, 1H), 7.01 (m, 1H) ppm.; ^{13}C NMR (75 MHz, CDCl_3) δ 57.3, 76.8, 77.5, 103.9 (dd, $^2J_{FC}$, $^3J_{FC} = 42.8, 1.5$ Hz), 107.9 (dd, $^2J_{FC}$, $^3J_{FC} = 23.3, 6.8$ Hz), 116.5 (dd, $^2J_{FC}$, $^3J_{FC} = 21.0, 10.5$ Hz), 146.1 (dd, $^2J_{FC}$, $^3J_{FC} = 13.6, 11.9$ Hz), 149.3 (dd, $^1J_{FC}$, $^4J_{FC} = 240.8, 3.8$ Hz), 158.6 (dd, $^1J_{FC}$, $^4J_{FC} = 240.8, 2.3$ Hz) ppm.; ^{19}F NMR (282 MHz, CDCl_3) δ -117.3 (d, $J_{FF} = 14.1$ Hz, 1F), -140.2 (d, $J_{FF} = 14.1$ Hz, 1F) ppm.

1,3-difluoro-2-(prop-2-yn-1-yloxy)benzene (5q) [63]

Purification by silica gel column chromatography using *n*-hexane as eluent gave colorless oil with 96% yield. ^1H NMR (300 MHz, CDCl_3) δ 2.51 (t, $J = 2.4$ Hz, 1H), 4.81 (d, $J = 2.4$ Hz, 2H), 6.96 (m, 3H) ppm.; ^{13}C NMR (75 MHz, CDCl_3) δ 61.6 (t, $^4J_{FC} = 3.8$ Hz), 76.3, 77.9, 112.2 (dd, $^2J_{FC}$, $^4J_{FC} = 15.0, 6.8$ Hz), 123.9 (t, $^3J_{FC} = 9.0$ Hz), 133.9 (t, $^3J_{FC} = 14.3$ Hz), 156.5 (dd, $^1J_{FC}$, $^3J_{FC} = 247.5, 5.3$ Hz) ppm.; ^{19}F NMR (282 MHz, CDCl_3) δ -128.1 (s, 2F) ppm.

1,2-difluoro-4-(prop-2-yn-1-yloxy)benzene (5r) [64]

Purification by silica gel column chromatography using *n*-hexane as eluent gave colorless oil with 88% yield. ^1H NMR (300 MHz, CDCl_3) δ 2.54 (t, $J = 2.4$ Hz, 1H), 4.65 (d, $J = 2.4$ Hz, 2H), 6.69 (m, 1H), 6.82 (m, 1H), 7.08 (m, 1H) ppm.; ^{13}C NMR (75 MHz, CDCl_3) δ 56.6, 76.1, 77.9, 104.9 (d, $^2J_{FC} = 20.3$ Hz), 110.4 (dd, $^2J_{FC} = 63.8$ Hz), 117.3 (dd, $^3J_{FC}$, $^4J_{FC} = 18.0, 1.5$ Hz), 148.0 (dd, $^1J_{FC}$, $^2J_{FC} = 240.0, 12.8$ Hz), 150.4 (dd, $^1J_{FC}$, $^2J_{FC} = 246.8, 14.3$ Hz), 153.7 (dd, $^3J_{FC}$, $^4J_{FC} = 9.0, 2.3$ Hz) ppm.; ^{19}F NMR (282 MHz, CDCl_3) δ -136.0 (d, $J_{FF} = 19.7$ Hz, 1F), -147.9 (d, $J_{FF} = 22.6$ Hz, 1F) ppm.

1,3-difluoro-5-(prop-2-yn-1-yloxy)benzene (5s) [62]

Purification by silica gel column chromatography using *n*-hexane as eluent gave colorless oil with 82% yield. ^1H NMR (300 MHz, CDCl_3) δ 2.56 (t, $J = 2.4$ Hz, 1H), 4.67 (d, $J = 2.4$ Hz, 2H), 6.45 (m, 1H), 6.52 (m, 2H) ppm.; ^{13}C NMR (75 MHz, CDCl_3) δ 56.3, 76.4, 77.5, 97.2 (t, $^2J_{FC} = 25.70$ Hz), 98.9 (dd, $^2J_{FC}$, $^4J_{FC} = 27.8, 0.8$ Hz), 159.4 (t, $^3J_{FC} = 13.6$ Hz), 163.6 (dd, $^1J_{FC}$, $^3J_{FC} = 245.3, 15.4$ Hz) ppm.; ^{19}F NMR (282 MHz, CDCl_3) δ -109.7 (s, 2F) ppm.

1-(prop-2-yn-1-yloxy)-3,5-bis(trifluoromethyl)benzene (5t)

Purification by silica gel column chromatography using *n*-hexane as eluent gave colorless oil with quantitative yield. ^1H NMR (300 MHz, CDCl_3) δ 2.59 (t, $J = 2.4$ Hz, 1H), 4.80 (d, $J = 2.4$ Hz, 2H), 7.40 (s, 2H), 7.52 (s, 1H) ppm.; ^{13}C NMR (75 MHz, CDCl_3) δ 56.2, 76.6, 76.9, 115.2 (m), 115.5 (d, $^4J_{FC} = 3.0$ Hz), 123.1 (q, $^1J_{FC} = 271.0$ Hz), 132.9 (q, $^2J_{FC} = 33.3$ Hz), 158.0 ppm.; ^{19}F NMR (282 MHz, CDCl_3) δ -63.2 (s, 6F) ppm.

1-chloro-4-(prop-2-yn-1-yloxy)-2-(trifluoromethyl)benzene (5u)

Purification by silica gel column chromatography using *n*-hexane as eluent gave colorless oil with 93% yield. ^1H NMR (300 MHz, CDCl_3) δ 2.56 (t, $J = 2.4$ Hz, 1H), 4.72 (d, $J = 2.4$ Hz, 2H), 7.09 (dd, $J = 8.8, 3.0$ Hz, 1H), 7.30 (d, $J = 3.0$ Hz, 1H), 7.42 (d, $J = 8.8$ Hz, 1H) ppm.; ^{13}C NMR (75 MHz, CDCl_3) δ 56.3, 76.5, 77.4, 114.7 (q, $^3J_{FC} = 5.3$ Hz), 119.1, 122.6 (q, $^1J_{FC} = 271.5$ Hz), 124.3, 129.2 (q, $^2J_{FC} = 30.8$ Hz),

132.4, 155.9 ppm.; ^{19}F NMR (282 MHz CDCl_3) δ -63.5 (s, 3F) ppm.

1-methyl-4-(prop-2-yn-1-yloxy)benzene (5v) [65]

Purification by silica gel column chromatography using *n*-hexane as eluent gave pale-yellow oil with 93% yield. ^1H NMR (300 MHz, CDCl_3) δ 2.29 (s, 3H), 2.50 (t, $J = 2.4$ Hz, 1H), 4.61 (d, $J = 2.4$ Hz, 2H), 6.83 (d, $J = 9.3$ Hz, 2H), 6.92 (d, $J = 9.3$ Hz, 2H) ppm.; ^{13}C NMR (75 MHz, $\text{DMSO}-d_6$) δ 20.5, 55.9, 75.3, 78.8, 114.8, 129.9, 130.9, 155.4 ppm.

1-ethyl-4-(prop-2-yn-1-yloxy)benzene (5w) [66]

Purification by silica gel column chromatography using *n*-hexane as eluent gave colorless oil with quantitative yield. ^1H NMR (300 MHz, CDCl_3) δ 1.21 (t, $J = 7.6$ Hz, 3H), 2.49 (t, $J = 2.4$ Hz, 1H), 2.59 (q, $J = 7.6$ Hz, 2H), 4.65 (d, $J = 2.4$ Hz, 2H), 6.90 (d, $J = 8.7$ Hz, 2H), 7.2 (d, $J = 8.7$ Hz, 2H) ppm.; ^{13}C NMR (75 MHz, $\text{DMSO}-d_6$) δ 15.8, 28.0, 55.9, 75.3, 78.8, 114.8, 128.7, 137.4, 155.6 ppm.

1-isopropyl-4-(prop-2-yn-1-yloxy)benzene (5x) [67]

Purification by silica gel column chromatography using *n*-hexane as eluent gave colorless oil with quantitative yield. ^1H NMR (300 MHz, CDCl_3) δ 1.23 (d, $J = 6.9$ Hz, 6H), 2.50 (t, $J = 2.4$ Hz, 1H), 2.86 (m, 1H), 4.66 (d, $J = 2.4$ Hz, 2H), 6.91 (d, $J = 8.7$ Hz, 2H), 7.16 (d, $J = 8.7$ Hz, 2H) ppm.; ^{13}C NMR (75 MHz, CDCl_3) δ 24.2, 33.3, 55.86, 75.3, 78.5, 114.7, 127.3, 142.0, 155.6 ppm.

1-chloro-4-(prop-2-yn-1-yloxy)benzene (5y) [65]

Purification by silica gel column chromatography using 5% EtOAc: *n*-hexane as eluent gave colorless oil with 70% yield. ^1H NMR (300 MHz, CDCl_3) δ 2.52 (t, $J = 2.4$ Hz, 1H), 4.66 (d, $J = 2.4$ Hz, 2H), 6.89 (d, $J = 9.1$ Hz, 2H), 7.24 (d, $J = 9.1$, 2H) ppm.; ^{13}C NMR (75 MHz, CDCl_3) δ 56.1, 75.8, 78.2, 116.3, 126.5, 129.4, 156.1 ppm.

1-bromo-4-(prop-2-yn-1-yloxy)benzene (5z) [68]

Purification by silica gel column chromatography using *n*-hexane as eluent gave colorless oil with 94% yield. ^1H NMR (300 MHz, CDCl_3) δ 2.52 (t, $J = 3.0$ Hz, 1H), 4.65 (d, $J = 3.0$ Hz, 2H), 6.86 (d, $J = 9.1$ Hz, 2H), 7.39 (d, $J = 9.1$ Hz, 2H) ppm.; ^{13}C NMR (75 MHz, CDCl_3) δ 55.9, 75.9, 78.1, 113.9, 116.7, 132.3, 156.6 ppm.

tert-butyl dimethyl(4-(prop-2-yn-1-yloxy)phenoxy)silane (5aa) [69]

Purification by silica gel column chromatography using 5% EtOAc: *n*-hexane as eluent gave white solid with 93% yield. ^1H NMR (300 MHz, CDCl_3) δ 0.17 (s, 6H), 0.98 (s, 9H), 2.50 (t, $J = 2.4$ Hz, 1H), 4.63 (d, $J = 2.4$ Hz, 2H), 6.77 (d, $J = 9.2$ Hz, 2H), 6.86 (d, $J = 9.2$ Hz, 2H) ppm.; ^{13}C NMR (75 MHz, CDCl_3) δ -4.1, 18.4, 25.9, 56.7, 75.4, 79.1, 116.1, 120.1, 150.4, 152.3 ppm.

1-methoxy-4-(prop-2-yn-1-yloxy)benzene (5ab) [63]

Purification by silica gel column chromatography using 5% EtOAc: *n*-hexane as eluent gave pale-yellow oil with 93% yield. ^1H NMR (300 MHz, CDCl_3) δ 2.50 (t, $J = 2.4$ Hz, 1H), 3.75 (s, 3H), 4.61 (d, $J = 2.4$ Hz, 2H), 6.83 (d, $J = 9.3$ Hz, 2H), 6.92 (d, $J = 9.3$ Hz, 2H) ppm.; ^{13}C NMR (75 MHz, CDCl_3) δ 55.6, 56.6, 75.3, 78.9, 114.6, 116.1, 151.7, 154.5 ppm.

N-(4-(prop-2-yn-1-yloxy)phenyl)acetamide (5ac) [70]

Purification by silica gel column chromatography using 30% EtOAc: *n*-hexane as eluent gave colorless oil with 98% yield. ^1H NMR (300 MHz, CDCl_3) δ 2.12 (s, 3H), 2.52 (t, $J = 2.3$ Hz, 1H), 4.65 (d, $J = 2.3$ Hz, 2H), 6.90 (d, $J = 8.9$ Hz, 2H), 7.80 (br s, 1H) ppm.; ^{13}C NMR (75 MHz, CDCl_3) δ 24.2, 56.1, 75.6, 78.5, 115.3, 121.9, 131.9, 154.3, 168.7 ppm.

4.3.2. Preparation of triazolyl phenols 7

General procedure B: Cycloaddition of alkynes 5 and azide 6 to 1,2,3-triazoles 7a-7ac [42]

To a stirred mixture of alkyne derivatives 5 and 4-azidophenol (6) in *n*-BuOH:water was added sodium ascorbate and 1 M aq. CuSO_4 , sequentially, at room temperature. The obtained mixture was stirred at 60 °C for 2–24 h. After that, the resulting solution was cooled down with ice water, followed by addition of 10% aq. NH_3 . It was then stirred for another 5 min. The formed precipitate was collected by a Büchner filtration. Purification of the crude products was performed by silica gel column chromatography to provide the desired products 7a-7ac.

4-(4-(phenoxy methyl)-1H-1,2,3-triazol-1-yl)phenol (7a) [42]

Purification by silica gel column chromatography using 50% EtOAc: *n*-hexane as eluent gave white solid with 62% yield. ¹H NMR (300 MHz, DMSO-*d*₆) δ 5.21 (s, 2H), 6.91–7.68 (m, 9H), 8.75 (s, 1H) ppm.; ¹³C NMR (75 MHz, DMSO-*d*₆) δ 61.0, 114.7, 116.1, 120.9, 122.0, 122.7, 129.2, 129.9, 143.5, 157.8, 158.0 ppm.

4-(4-(2-fluorophenoxy)methyl)-1H-1,2,3-triazol-1-yl)phenol (7b) [42]

Purification by silica gel column chromatography using 50% EtOAc: *n*-hexane as eluent gave brown solid with 57% yield. ¹H NMR (300 MHz, DMSO-*d*₆) δ 5.29 (s, 2H), 6.95 (d, *J* = 8.9 Hz, 2H), 6.95–7.01 (m, 1H), 7.13–7.19 (m, 1H), 7.23 (dd, *J* = 8.9, 1.6 Hz, 1H), 7.40 (td, *J* = 8.5, 1.5 Hz, 1H), 7.69 (d, *J* = 8.9, 2H), 8.79 (s, 1H), 9.98 (br s, 1H) ppm.; ¹³C NMR (75 MHz, DMSO-*d*₆) δ 62.0, 115.6, 116.1 (d, ²*J*_{FC} = 18.0 Hz), 116.1, 121.5 (d, ³*J*_{FC} = 7.5 Hz), 122.1, 123.0, 124.8 (d, ³*J*_{FC} = 3.8 Hz), 128.7, 143.0, 145.9 (d, ²*J*_{FC} = 10.4 Hz), 151.8 (d, ¹*J*_{FC} = 242.0 Hz), 157.9 ppm.; ¹⁹F NMR (282 MHz, DMSO-*d*₆) δ –136.4 (s, 1F) ppm.; HRMS (ESI+) *m/z*: calcd. for C₁₅H₁₃FN₃O₂ [M+H]⁺ 286.0992, found 286.0987.

4-(4-(3-fluorophenoxy)methyl)-1H-1,2,3-triazol-1-yl)phenol (7c) [42]

Purification by silica gel column chromatography using 50% EtOAc: *n*-hexane as eluent gave brown solid with 81% yield. ¹H NMR (300 MHz, DMSO-*d*₆) δ 5.23 (s, 1H), 6.78 (td, *J* = 8.67, 2.37 Hz, 1H), 6.94 (m, 4H), 7.32 (m, 1H), 7.67 (d, *J* = 8.9 Hz, 2H), 8.75 (s, 1H), 9.97 (br s, 1H) ppm.; ¹³C NMR (75 MHz, DMSO-*d*₆) δ 61.5, 102.4, (d, ²*J*_{FC} = 24.8 Hz), 107.7 (d, ²*J*_{FC} = 21.0 Hz), 111.2 (d, ⁴*J*_{FC} = 3.0 Hz), 116.2, 122.2, 123.0, 128.8, 130.8 (d, ³*J*_{FC} = 10.5 Hz), 143.2, 158.0, 159.6 (d, ³*J*_{FC} = 11.3 Hz), 163.1 (d, ¹*J*_{FC} = 241.5 Hz) ppm.; ¹⁹F NMR (282 MHz, DMSO-*d*₆) δ –113.0 (s, 1F) ppm.; HRMS (ESI+) *m/z*: calcd. for C₁₅H₁₃FN₃O₂ [M+H]⁺ 308.0809, found 308.0811.

4-(4-(4-fluorophenoxy)methyl)-1H-1,2,3-triazol-1-yl)phenol (7d) [42]

Purification by silica gel column chromatography using 50% EtOAc: *n*-hexane as eluent gave white solid with 62% yield. ¹H NMR (300 MHz, DMSO-*d*₆) δ 5.18 (s, 2H), 6.94 (dd, *J* = 6.0, 3.0 Hz, 2H), 7.12 (m, 4H), 7.66 (dd, *J* = 6.0, 3.0 Hz, 2H), 8.75 (3, 1H), 9.96 (br s, 1H) ppm.; ¹³C NMR (75 MHz, DMSO-*d*₆) δ 61.6, 115.9 (d, ²*J*_{FC} = 25.1 Hz), 116.1 (d, ³*J*_{FC} = 10.1 Hz), 116.1, 122.0, 122.8, 128.7, 143.4, 154.3 (d, ⁴*J*_{FC} = 1.8 Hz), 156.7 (d, ¹*J*_{FC} = 234.6 Hz), 157.8 ppm.; ¹⁹F NMR (282 MHz, DMSO-*d*₆) δ –125.2 (s, 1F) ppm.; HRMS (ESI+) *m/z*: calcd. for C₁₅H₁₃FN₃O₂ [M+H]⁺ 286.0992, found 286.0981.

4-(4-(2-nitrophenoxy)methyl)-1H-1,2,3-triazol-1-yl)phenol (7e) [42]

Purification by silica gel column chromatography using 50% EtOAc: *n*-hexane as eluent gave brown solid with 80% yield. ¹H NMR (300 MHz, DMSO-*d*₆) δ 5.43 (s, 2H), 6.94 (dd, *J* = 10.0, 3.3 Hz, 2H), 7.15 (ddd, *J* = 8.0, 7.2, 1.4 Hz, 1H), 7.67 (m, 4H), 7.88 (dd, *J* = 8.1, 1.6 Hz, 1H), 8.77 (s, 1H), 9.98 (br s, 1H) ppm.; ¹³C NMR (75 MHz, DMSO-*d*₆) δ 62.5, 115.7, 116.1, 121.1, 122.1, 123.1, 125.0, 128.6, 134.4, 139.9, 142.2, 150.6, 157.9 ppm.; HRMS (ESI+) *m/z*: calcd. for C₁₆H₁₃F₃N₃O₂ [M+H]⁺ 313.0937, found 313.0937.

4-(4-(3-nitrophenoxy)methyl)-1H-1,2,3-triazol-1-yl)phenol (7f) [42]

Purification by silica gel column chromatography using 50% EtOAc: *n*-hexane as eluent gave brown solid with 96% yield. ¹H NMR (300 MHz, DMSO-*d*₆) δ 5.38 (s, 2H), 6.95 (dd, *J* = 12.3, 5.5 Hz, 2H), 7.62 (m, 4H), 7.85 (ddd, *J* = 7.7, 2.1, 1.2 Hz, 1H), 7.91 (t, *J* = 2.1 Hz, 1H), 8.80 (s, 1H), 9.98 (br s, 1H) ppm.; ¹³C NMR (75 MHz, DMSO-*d*₆) δ 61.8, 109.2, 115.9, 116.1, 122.1, 122.2, 123.0, 128.7, 130.8, 142.8, 142.8, 157.9, 158.5 ppm.; HRMS (ESI+) *m/z*: calcd. for C₁₅H₁₃N₄O₄ [M+H]⁺ 313.0937, found 313.0927.

4-(4-(4-nitrophenoxy)methyl)-1H-1,2,3-triazol-1-yl)phenol (7g) [42]

Purification by silica gel column chromatography using 50% EtOAc: *n*-hexane as eluent gave brown solid with 63% yield. ¹H NMR (300 MHz,

DMSO-*d*₆) δ 5.40 (s, 2H), 6.95 (d, *J* = 9.0 Hz, 2H), 7.31 (d, *J* = 9.0 Hz, 2H), 7.68 (d, *J* = 9.0 Hz, 2H), 8.24 (d, *J* = 9.0 Hz, 2H), 8.81 (s, 1H), 9.99 (br s, 1H) ppm.; ¹³C NMR (75 MHz, DMSO-*d*₆) δ 61.9, 115.4, 116.1, 122.1, 123.1, 125.9, 128.6, 141.1, 142.5, 157.9, 163.2 ppm.; HRMS (ESI+) *m/z*: calcd. for C₁₅H₁₃N₄O₄ [M+H]⁺ 313.0937, found 313.0936.

4-(4-(2-(trifluoromethyl)phenoxy)methyl)-1H-1,2,3-triazol-1-yl)phenol (7h)

Purification by silica gel column chromatography using 50% EtOAc: *n*-hexane as eluent gave brown solid with 66% yield. Mp. = 171–173 °C; ¹H NMR (300 MHz, DMSO-*d*₆) δ 5.37 (s, 2H), 6.94 (d, *J* = 8.9 Hz, 2H), 7.11 (t, *J* = 7.5 Hz, 1H), 7.52 (d, *J* = 8.4 Hz, 1H), 7.65 (m, 4H), 8.72 (s, 1H), 9.94 (br s, 1H) ppm.; ¹³C NMR (75 MHz, DMSO-*d*₆) δ 62.0, 114.3, 116.2, 117.5 (q, ²*J*_{FC} = 15.0 Hz), 123.8 (q, ¹*J*_{FC} = 270.8 Hz), 120.8, 122.1, 122.9, 126.9 (q, ³*J*_{FC} = 5.3 Hz), 128.7, 134.3, 143.0, 155.9, 158.0 ppm.; ¹⁹F NMR (282 MHz, DMSO-*d*₆) δ –62.3 (s, 3F) ppm.; HRMS (ESI+) *m/z*: calcd for C₁₆H₁₂F₃N₃O₂Na [M+Na]⁺ 358.0779, found 358.0774.

4-(4-(3-(trifluoromethyl)phenoxy)methyl)-1H-1,2,3-triazol-1-yl)phenol (7i)

Purification by silica gel column chromatography using 50% EtOAc: *n*-hexane as eluent gave brown solid with 39% yield. Mp. = 184–186 °C; ¹H NMR (300 MHz, DMSO-*d*₆) δ 5.32 (s, 2H), 6.95 (d, *J* = 8.9 Hz, 2H), 7.32 (d, *J* = 7.7 Hz, 1H), 7.40 (d, *J* = 7.1 Hz, 2H), 7.56 (m, 1H), 7.67 (d, *J* = 8.9 Hz, 2H), 8.78 (s, 1H), 9.96 (br s, 1H) ppm.; ¹³C NMR (75 MHz, DMSO-*d*₆) δ 61.5, 111.5 (q, ³*J*_{FC} = 3.8 Hz), 116.2, 117.6 (q, ³*J*_{FC} = 3.8 Hz), 119.1, 122.1, 124.2 (q, ¹*J*_{FC} = 270.0 Hz), 122.1, 123.0, 128.7, 130.5 (q, ²*J*_{FC} = 31.5 Hz), 143.1, 157.9, 158.4 ppm.; ¹⁹F NMR (282 MHz, DMSO-*d*₆) δ –62.7 (s, 3F) ppm.; HRMS (ESI+) *m/z*: calcd for C₁₆H₁₃F₃N₃O₂ [M+H]⁺ 336.0960, found 336.0954.

4-(4-(4-(trifluoromethyl)phenoxy)methyl)-1H-1,2,3-triazol-1-yl)phenol (7j)

Purification by silica gel column chromatography using 50% EtOAc: *n*-hexane as eluent gave pale-pink solid with 82% yield. Mp. = 225–226 °C; ¹H NMR (300 MHz, DMSO-*d*₆) δ 5.32 (s, 2H), 6.95 (d, *J* = 8.9 Hz, 2H), 7.26 (d, *J* = 8.9 Hz, 2H), 7.67 (m, 4H), 8.79 (s, 1H), 9.98 (br s, 1H) ppm.; ¹³C NMR (75 MHz, DMSO-*d*₆) δ 61.4, 115.4, 116.2, 124.7 (q, ¹*J*_{FC} = 270.0 Hz), 121.6 (q, ²*J*_{FC} = 31.9 Hz) 122.2, 123.1, 127.12 (q, ³*J*_{FC} = 3.5 Hz), 128.8, 123.1, 158.0, 160.9 ppm.; ¹⁹F NMR (282 MHz, DMSO-*d*₆) δ –61.4 (s, 3F) ppm.; HRMS (ESI+) *m/z*: calcd for C₁₆H₁₂F₃N₃O₂Na [M+Na]⁺ 358.0779, found 358.0777.

4-(4-(2-(tert-butyl)phenoxy)methyl)-1H-1,2,3-triazol-1-yl)phenol (7k)

Purification by silica gel column chromatography using 50% EtOAc: *n*-hexane as eluent gave brown solid with 48% yield. Mp. = 226–227 °C; ¹H NMR (300 MHz, DMSO-*d*₆) δ 1.31 (s, 9H), 5.23 (s, 2H), 6.91 (m, 1H), 6.96 (d, *J* = 8.9 Hz, 2H), 7.23 (m, 3H), 7.79 (d, *J* = 8.9 Hz, 2H), 8.76 (s, 1H), 9.97 (br s, 1H) ppm.; ¹³C NMR (75 MHz, DMSO-*d*₆) δ 29.7, 34.4, 61.1, 113.0, 116.1, 120.7, 122.0, 122.4, 126.3, 127.2, 128.7, 137.5, 143.7, 156.9, 157.8 ppm.; HRMS (ESI+) *m/z*: calcd for C₁₉H₂₂N₃O₂ [M+H]⁺ 324.1712, found 324.1697.

4-(4-(3-(tert-butyl)phenoxy)methyl)-1H-1,2,3-triazol-1-yl)phenol (7l)

Purification by silica gel column chromatography using 50% EtOAc: *n*-hexane as eluent gave brown solid with 47% yield. Mp. = 171–172 °C; ¹H NMR (300 MHz, DMSO-*d*₆) δ 1.52 (s, 9H), 5.19 (s, 2H), 6.95 (m, 5H), 7.23 (t, *J* = 7.9 Hz, 1H), 7.67 (d, *J* = 8.9 Hz, 2H), 8.74 (s, 1H), 9.94 (br s, 1H) ppm.; ¹³C NMR (75 MHz, DMSO-*d*₆) δ 31.1, 34.5, 61.0, 111.2, 112.5, 116.2, 117.9, 122.1, 122.7, 128.8, 129.1, 143.9, 152.5, 157.9, 158.0 ppm.; HRMS (ESI+) *m/z*: calcd for C₁₉H₂₁N₃O₂Na [M+Na]⁺ 346.1531, found 346.1528.

4-(4-(4-(tert-butyl)phenoxy)methyl)-1H-1,2,3-triazol-1-yl)phenol (7m)

Purification by silica gel column chromatography using 50% EtOAc: *n*-hexane as eluent gave pale-pink solid with 26% yield. Mp. = 237–238 °C; ¹H NMR (300 MHz, DMSO-*d*₆) δ 1.25 (s, 9H), 5.17 (s, 2H), 6.96 (m, 4H), 7.31 (d, *J* = 8.7 Hz, 2H), 7.67 (d, *J* = 8.7 Hz, 2H), 8.74 (s,

1H), 9.96 (br s, 1H) ppm.; ¹³C NMR (75 MHz, DMSO-*d*₆) δ 31.3, 33.8, 61.0, 114.2, 116.0, 122.0, 122.6, 126.1, 128.7, 143.1, 143.7, 155.8, 157.8 ppm.; HRMS (ESI+) *m/z*: calcd for C₁₉H₂₂N₃O₂ [M+H]⁺ 324.1712, found 324.1715.

4-(4-((2,3-difluorophenoxy)methyl)-1H-1,2,3-triazol-1-yl)phenol (7n)

Purification by silica gel column chromatography using 50% EtOAc: *n*-hexane as eluent gave brown solid with 68% yield. Mp. = 185–187 °C; ¹H NMR (300 MHz, DMSO-*d*₆) δ 5.33 (s, 2H), 6.94 (d, *J* = 8.9 Hz, 2H), 7.01 (m, 1H), 7.16 (m, 1H), 7.26 (m, 1H), 7.67 (d, *J* = 8.9 Hz, 2H), 8.78 (s, 1H), 9.96 (br s, 1H) ppm.; ¹³C NMR (75 MHz, DMSO-*d*₆) δ 62.5, 109.4 (d, ³*J*_{FC} = 16.5 Hz), 111.1 (d, ³*J*_{FC} = 3.0 Hz), 116.2, 122.2, 123.2, 124.2 (dd, ²*J*_{FC}, ³*J*_{FC} = 9.0, 5.3 Hz), 128.7, 140.4 (dd, ¹*J*_{FC}, ²*J*_{FC} = 243.8, 14.3 Hz), 142.8, 147.5 (dd, ²*J*_{FC}, ³*J*_{FC} = 7.5, 3.1 Hz), 150.6 (dd, ¹*J*_{FC}, ²*J*_{FC} = 242.3, 9.3 Hz), 158.0 ppm.; ¹⁹F NMR (282 MHz, DMSO-*d*₆) δ -139.8 (s, 1F), -139.9 (s, 1F) ppm.; HRMS (ESI+) *m/z*: calcd for C₁₅H₁₁F₂N₃O₂Na [M+Na]⁺ 326.0717, found 326.0716.

4-(4-((2,4-difluorophenoxy)methyl)-1H-1,2,3-triazol-1-yl)phenol (7o)

Purification by silica gel column chromatography using 50% EtOAc: *n*-hexane as eluent gave brown solid with 64% yield. Mp. = 183–184 °C; ¹H NMR (300 MHz, DMSO-*d*₆) δ 5.27 (s, 2H), 6.94 (d, *J* = 8.9 Hz, 2H), 7.02 (m, 1H), 7.27 (m, 1H), 7.40 (m, 1H), 7.66 (d, *J* = 8.9 Hz, 2H) ppm.; ¹³C NMR (75 MHz, DMSO-*d*₆) δ 62.7, 105.0 (dd, ²*J*_{FC}, ²*J*_{FC} = 68.3, 22.5 Hz), 110.9 (dd, ²*J*_{FC}, ⁴*J*_{FC} = 21.8, 3.8 Hz), 116.16, 115.53 (dd, ³*J*_{FC}, ³*J*_{FC} = 9.0, 2.3 Hz), 122.2, 123.1, 128.8, 142.6 (dd, ²*J*_{FC}, ⁴*J*_{FC} = 10.5, 3.8 Hz), 143.0, 151.69 (dd, ¹*J*_{FC}, ³*J*_{FC} = 245.3, 10.5 Hz), 155.9 (dd, ¹*J*_{FC}, ³*J*_{FC} = 237.8, 10.5 Hz), 158.0 ppm.; ¹⁹F NMR (282 MHz, DMSO-*d*₆) δ -121.3 (d, *J*_{FF} = 28.2 Hz, 1F), -131.1 (d, *J*_{FF} = 28.2 Hz, 1F) ppm.; HRMS (ESI+) *m/z*: calcd for C₁₅H₁₁F₂N₃O₂Na [M+Na]⁺ 326.0717, found 326.0719.

4-(4-((2,5-difluorophenoxy)methyl)-1H-1,2,3-triazol-1-yl)phenol (7p)

Purification by silica gel column chromatography using 50% EtOAc: *n*-hexane as eluent gave brown solid with 73% yield. Mp. = 180–181 °C; ¹H NMR (300 MHz, DMSO-*d*₆) δ 5.31 (s, 2H), 6.78 (m, 1H), 6.95 (d, *J* = 9.0 Hz, 2H), 7.25 (m, 1H), 7.36 (m, 1H), 7.68 (d, *J* = 9.0 Hz, 2H), 8.78 (s, 1H), 9.98 (br s, 1H) ppm.; ¹³C NMR (75 MHz, DMSO-*d*₆) δ 62.3, 103.5 (dd, ²*J*_{FC}, ³*J*_{FC} = 27.8, 2.3 Hz), 107.0 (dd, ²*J*_{FC}, ³*J*_{FC} = 24.0, 17.5 Hz), 116.2, 116.6 (dd, ²*J*_{FC}, ³*J*_{FC} = 20.3, 10.5 Hz), 122.2, 123.3, 128.7, 142.6, 146.7 (dd, ²*J*_{FC}, ³*J*_{FC} = 12.0, 11.3 Hz), 148.3 (dd, ¹*J*_{FC}, ⁴*J*_{FC} = 242.3, 3.0 Hz), 158.3 (dd, ¹*J*_{FC}, ⁴*J*_{FC} = 238.5, 2.3 Hz), 158.0 ppm.; ¹⁹F NMR (282 MHz, DMSO-*d*₆) δ -117.5 (d, *J*_{FF} = 15.2 Hz, 1F), -141.3 (d, *J*_{FF} = 15.2 Hz, 1F) ppm.; HRMS (ESI+) *m/z*: calcd for C₁₅H₁₁F₂N₃O₂Na [M+Na]⁺ 326.0717, found 326.0718.

4-(4-((2,6-difluorophenoxy)methyl)-1H-1,2,3-triazol-1-yl)phenol (7q)

Purification by silica gel column chromatography using 50% EtOAc: *n*-hexane as eluent gave brown solid with 50% yield. Mp. = 166–168 °C; ¹H NMR (300 MHz, DMSO-*d*₆) δ 5.26 (s, 2H), 6.94 (d, *J* = 9.0 Hz, 2H), 7.10 (m, 3H), 7.65 (d, *J* = 9.0 Hz, 2H), 8.73 (s, 1H), 9.94 (br s, 1H) ppm.; ¹³C NMR (75 MHz, DMSO-*d*₆) δ 66.6 (t, ⁴*J*_{FC} = 3.0 Hz), 112.6 (dd, ³*J*_{FC}, ³*J*_{FC} = 8.3, 6.8 Hz), 116.2, 122.0, 123.1, 124.3 (t, ³*J*_{FC} = 9.0 Hz), 128.7, 134.0 (t, ²*J*_{FC} = 14.3 Hz), 143.0, 155.8 (dd, ¹*J*_{FC}, ³*J*_{FC} = 245.3, 5.3 Hz), 157.9 ppm.; ¹⁹F NMR (282 MHz, DMSO-*d*₆) δ -129.2 (s, 2F) ppm.; HRMS (ESI+) *m/z*: calcd for C₁₅H₁₁F₂N₃O₂Na [M+Na]⁺ 326.0717, found 326.0719.

4-(4-((3,4-difluorophenoxy)methyl)-1H-1,2,3-triazol-1-yl)phenol (7r)

Purification by silica gel column chromatography using 50% EtOAc: *n*-hexane as eluent gave brown solid with 80% yield. Mp. = 195–197 °C; ¹H NMR (300 MHz, DMSO-*d*₆) δ 5.20 (s, 2H), 6.89 (m, 1H), 6.94 (d, *J* = 8.8 Hz, 2H), 7.21 (ddd, *J* = 12.5, 6.7, 2.8 Hz, 1H), 7.34 (q, *J* = 9.7 Hz, 1H), 7.66 (d, *J* = 8.7 Hz, 2H), 8.74 (s, 1H), 9.95 (br s, 1H) ppm.; ¹³C NMR (75 MHz, DMSO-*d*₆) δ 61.9, 104.5 (d, ²*J*_{FC} = 20.3 Hz), 111.2 (dd, ²*J*_{FC}, ³*J*_{FC} = 5.9, 3.2 Hz), 116.2, 117.7 (d, ³*J*_{FC} = 18.8 Hz), 122.2, 123.0, 128.8, 144.3 (dd, ¹*J*_{FC}, ²*J*_{FC} = 236.3, 12.8 Hz), 149.7 (dd, ¹*J*_{FC}, ²*J*_{FC} =

243.8, 13.5 Hz), 154.7 (dd, ²*J*_{FC}, ³*J*_{FC} = 8.9, 1.5 Hz), 158.0 ppm.; ¹⁹F NMR (282 MHz, DMSO-*d*₆) δ -137.9 (d, *J*_{FF} = 22.8, 1F), -150.4 (d, *J*_{FF} = 22.8, 1F) ppm.; HRMS (ESI+) *m/z*: calcd for C₁₅H₁₁F₂N₃O₂Na [M+Na]⁺ 326.0717, found 326.0712.

4-(4-((3,5-difluorophenoxy)methyl)-1H-1,2,3-triazol-1-yl)phenol (7s)

Purification by silica gel column chromatography using 50% EtOAc: *n*-hexane as eluent gave brown solid with 77% yield. Mp. = 223–224 °C; ¹H NMR (300 MHz, DMSO-*d*₆) δ 5.26 (s, 2H), 6.84 (m, 3H), 6.95 (d, *J* = 8.9 Hz, 2H), 7.67 (d, *J* = 8.9 Hz, 2H), 8.79 (s, 1H), 9.97 (br s, 1H) ppm.; ¹³C NMR (75 MHz, DMSO-*d*₆) δ 61.9, 96.6 (t, ²*J*_{FC} = 26.3 Hz), 99.3 (dd, ²*J*_{FC}, ⁴*J*_{FC} = 18.9, 9.4 Hz), 116.2, 122.2, 123.1, 128.7, 142.7, 158.0, 160.2 (t, ³*J*_{FC} = 14.1 Hz), 163.1 (dd, ¹*J*_{FC}, ³*J*_{FC} = 242.6, 16.2 Hz) ppm.; ¹⁹F NMR (282 MHz, DMSO-*d*₆) δ -110.6 (s, 2F) ppm.; HRMS (ESI+) *m/z*: calcd for C₁₅H₁₁F₂N₃O₂ [M+H]⁺ 304.0898, found 304.0886.

4-(4-((3,5-bis(trifluoromethyl)phenoxy)methyl)-1H-1,2,3-triazol-1-yl)phenol (7t)

Purification by silica gel column chromatography using 50% EtOAc: *n*-hexane as eluent gave brown solid with 85% yield. Mp. = 199–200 °C; ¹H NMR (300 MHz, DMSO-*d*₆) δ 5.45 (s, 2H), 6.95 (d, *J* = 8.9 Hz, 2H), 7.67 (m, 2H), 7.79 (s, 2H), 8.80 (s, 1H), 9.98 (br s, 1H) ppm.; ¹³C NMR (75 MHz, DMSO-*d*₆) δ 62.1, 114.1, 116.0, 116.1, 123.1 (q, ¹*J*_{FC} = 270.8 Hz), 122.1, 123.1, 128.6, 131.6 (q, ²*J*_{FC} = 33.4 Hz), 142.6, 157.9, 159.0 ppm.; ¹⁹F NMR (282 MHz, DMSO-*d*₆) δ -62.9 (s, 6F) ppm.; HRMS (ESI+) *m/z*: calcd for C₁₇H₁₂F₆N₃O₂ [M+H]⁺ 404.0834, found 404.0838.

4-(4-((4-chloro-3-(trifluoromethyl)phenoxy)methyl)-1H-1,2,3-triazol-1-yl)phenol (7u)

Purification by silica gel column chromatography using 50% EtOAc: *n*-hexane as eluent gave brown solid with 41% yield. Mp. = 191–193 °C; ¹H NMR (300 MHz, DMSO-*d*₆) δ 5.45 (s, 2H), 6.95 (d, *J* = 8.9 Hz, 2H), 7.67 (m, 2H), 7.79 (s, 2H), 8.80 (s, 1H), 9.98 (br s, 1H) ppm.; ¹³C NMR (75 MHz, DMSO-*d*₆) δ 61.8, 114.6 (q, ³*J*_{FC} = 5.5 Hz), 116.1, 122.4 (q, ¹*J*_{FC} = 270.0 Hz), 120.2, 121.9 (d, ⁴*J*_{FC} = 2.3 Hz), 122.1, 123.0, 127.5 (q, ²*J*_{FC} = 25.5 Hz), 128.6, 132.8, 142.8, 156.8, 158.0 ppm.; ¹⁹F NMR (282 MHz, DMSO-*d*₆) δ -62.9 (s, 3F) ppm.; HRMS (ESI+) *m/z*: calcd for C₁₆H₁₃ClF₃N₃O₂ [M+H]⁺ 370.0570, found 370.0565.

4-(4-((*p*-tolylloxy)methyl)-1H-1,2,3-triazol-1-yl)phenol (7v) [44]

Purification by silica gel column chromatography using 50% EtOAc: *n*-hexane as eluent gave brown solid with 31% yield. ¹H NMR (300 MHz, CDCl₃) δ 2.24 (s, 3H), 5.16 (s, 2H), 7.00 (m, 8H), 8.74 (s, 1H), 9.97 (s, 1H) ppm.; ¹³C NMR (300 MHz, DMSO-*d*₆) δ 20.1, 61.0, 114.6, 116.0, 122.0, 122.6, 128.7, 128.6, 129.8, 143.6, 155.9, 157.8 ppm.

4-(4-((4-ethylphenoxy)methyl)-1H-1,2,3-triazol-1-yl)phenol (7w) [44]

Purification by silica gel column chromatography using 50% EtOAc: *n*-hexane as eluent gave brown solid with 25% yield. Mp. = 182–186 °C; ¹H NMR (300 MHz, DMSO-*d*₆) δ 1.15 (t, *J* = 7.6 Hz, 3H), 2.54 (q, *J* = 7.6 Hz, 2H), 5.17 (s, 2H), 6.97 (m, 4H), 7.14 (d, *J* = 8.6 Hz, 2H), 7.67 (d, *J* = 8.9 Hz, 2H), 8.74 (s, 1H), 9.93 (br s, 1H) ppm.; ¹³C NMR (75 MHz, DMSO-*d*₆) δ 15.9, 27.3, 61.1, 114.6, 116.1, 122.0, 122.6, 128.7, 128.8, 136.2, 143.7, 156.1, 157.8 ppm.; HRMS (ESI+) *m/z*: calcd for C₁₇H₁₈N₃O₂ [M+H]⁺ 296.1399, found 296.1395.

4-(4-((4-isopropylphenoxy)methyl)-1H-1,2,3-triazol-1-yl)phenol (7x) [44]

Purification by silica gel column chromatography using 50% EtOAc: *n*-hexane as eluent gave brown solid with 67% yield. Mp. = 214–215 °C; ¹H NMR (300 MHz, DMSO-*d*₆) δ 1.18 (d, *J* = 6.9, 6H), 2.83 (m, 1H), 5.17 (s, 2H), 6.65 (m, 4H), 7.17 (d, *J* = 8.7 Hz, 2H), 7.68 (d, *J* = 2.8 Hz, 2H), 8.75 (s, 1H) ppm.; ¹³C NMR (75 MHz, DMSO-*d*₆) δ 24.1, 32.6, 61.1, 114.6, 116.1, 122.0, 122.7, 127.2, 128.8, 140.9, 143.8, 156.2, 157.8 ppm.; HRMS (ESI+) *m/z*: calcd for C₁₈H₂₀N₃O₂ [M+H]⁺ 310.1556, found 310.1539.

4-(4-((4-chlorophenoxy)methyl)-1H-1,2,3-triazol-1-yl)phenol (7y)

Purification by silica gel column chromatography using 50% EtOAc:

n-hexane as eluent gave pale-pink solid with 53% yield. Mp. = 223–224 °C; ¹H NMR (300 MHz, DMSO-*d*₆) δ 5.21 (s, 2H), 6.94 (d, *J* = 9.0 Hz, 2H), 7.10 (d, *J* = 9.0 Hz, 2H), 7.35 (d, *J* = 9.0 Hz, 2H), 7.66 (d, *J* = 9.0 Hz, 2H), 8.75 (s, 1H), 9.96 (br s, 1H) ppm.; ¹³C NMR (75 MHz, DMSO-*d*₆) δ 61.4, 116.0, 116.6, 122.0, 122.8, 124.6, 128.7, 129.3, 143.2, 156.8, 157.8 ppm.; HRMS (ESI+) *m/z*: calcd for C₁₅H₁₃ClN₃O₂ [M+H]⁺ 302.0696, found 302.0688.

4-(4-((4-bromophenoxy)methyl)-1H-1,2,3-triazol-1-yl)phenol (7z)

Purification by silica gel column chromatography using 50% EtOAc: *n*-hexane as eluent gave brown solid with 87% yield. Mp. = 236–238 °C; ¹H NMR (300 MHz, DMSO-*d*₆) δ 5.21 (s, 2H), 6.94 (d, *J* = 8.9 Hz, 2H), 7.05 (d, *J* = 9.1 Hz, 2H), 7.47 (d, *J* = 9.1 Hz, 2H), 7.66 (d, *J* = 8.9 Hz, 2H), 8.75 (s, 1H), 10.01 (br s, 1H) ppm.; ¹³C NMR (75 MHz, DMSO-*d*₆) δ 61.3, 99.6, 112.5, 116.2, 117.2, 122.2, 123.0, 128.8, 132.3, 143.3, 157.9 ppm.; HRMS (ESI+) *m/z*: calcd for C₁₅H₁₃BrN₃O₂ [M+H]⁺ 346.0191, found 346.0197.

4-(4-(((tert-butyl)dimethylsilyloxy)phenoxy)methyl)-1H-1,2,3-triazol-1-yl)phenol (7aa)

Purification by silica gel column chromatography using 50% EtOAc: *n*-hexane as eluent gave white solid with 58% yield. Mp. = 217–220 °C; ¹H NMR (300 MHz, DMSO-*d*₆) δ 0.15 (s, 6H), 0.93 (s, 9H), 5.12 (s, 2H), 6.94 (d, *J* = 8.7 Hz, 2H), 6.98 (d, *J* = 8.7 Hz, 2H), 7.31 (d, *J* = 9.0 Hz), 7.67 (d, *J* = 9.0 Hz, 2H), 8.72 (s, 1H), 9.96 (s, 1H) ppm.; ¹³C NMR (75 MHz, DMSO-*d*₆) δ -4.6, 17.9, 25.6, 61.5, 115.7, 116.1, 120.5, 122.0, 122.6, 128.8, 143.7, 149.0, 151.5, 157.8 ppm.; HRMS (ESI+) *m/z*: calcd for C₂₁H₂₈N₃O₃Si [M+H]⁺ 398.1900, found 398.1883.

4-(4-((4-methoxyphenoxy)methyl)-1H-1,2,3-triazol-1-yl)phenol (7ab)

Purification by silica gel column chromatography using 50% EtOAc: *n*-hexane as eluent gave brown solid with 89% yield. Mp. = 193–195 °C; ¹H NMR (300 MHz, DMSO-*d*₆) δ 3.69 (s, 3H), 5.13 (s, 2H), 6.87 (d, *J* = 9.2 Hz, 2H), 6.97 (m, 4H), 7.67 (d, *J* = 8.8, 2H), 8.73 (s, 1H), 9.98 (br s, 1H) ppm.; ¹³C NMR (75 MHz, DMSO-*d*₆) δ 55.3, 61.6, 114.6, 115.7, 116.1, 120.0, 122.6, 128.8, 143.8, 152.0, 153.6, 157.8 ppm.; HRMS (ESI+) *m/z*: calcd for C₁₆H₁₆N₃O₃ [M+H]⁺ 298.1192, found 298.1184.

N-(4-(((1-(4-hydroxyphenyl)-1H-1,2,3-triazol-4-yl)methoxy)phenyl)acetamide (7ac)

Purification by silica gel column chromatography using 80% EtOAc: *n*-hexane as eluent gave brown solid with 82% yield. Mp. = 237–239 °C; ¹H NMR (300 MHz, DMSO-*d*₆) δ 2.01 (s, 3H), 3.63 (br s, 1H), 5.15 (s, 2H), 6.97 (m, 4H), 7.50 (d, *J* = 9.0 Hz, 2H), 7.66 (m, 2H), 8.12 (s, 1H), 9.82 (s, 1H) ppm.; ¹³C NMR (75 MHz, DMSO-*d*₆) δ 23.9, 61.3, 114.9, 116.2, 120.7, 122.1, 122.8, 128.8, 133.0, 143.7, 153.9, 157.9, 168.0 ppm.; HRMS (ESI+) *m/z*: calcd for C₁₇H₁₆F₃N₄O₃Na [M+Na]⁺ 347.1120, found 347.1124.

4.3.3. Synthesis of the target Sorafenib analogues 2

General procedure C: Synthesis of the triazole-containing Sorafenib analogues 2a-2ac [42]

To a stirred solution of triazole-containing phenol derivatives **7** in dried DMF was added 4-chloro-*N*-methylpicolinamide (**8**), *t*-BuOK and K₂CO₃. It was stirred under argon atmosphere at 80–85 °C for various times. The resulting mixture was cooled to room temperature, diluted with water and extracted with EtOAc. The combined organic phase was dried over anhydrous Na₂SO₄, filtered and concentrated under reduced pressure to obtain the crude product. It was purified by silica gel column chromatography to afford the desired products **2a-2ac**.

N-methyl-4-(4-(4-(phenoxy)methyl)-1H-1,2,3-triazol-1-yl)phenoxy)picolinamide (2a) [42]

Purification by silica gel column chromatography using 50% EtOAc: *n*-hexane as eluent gave white solid with 76% yield. ¹H NMR (300 MHz, CDCl₃) δ 3.20 (d, *J* = 6.0 Hz, 3H), 5.33 (s, 2H), 7.02 (m, 4H), 7.31 (m, 5H), 7.76 (d, *J* = 2.5 Hz, 1H), 7.78 (d, *J* = 9.0 Hz, 2H), 8.06 (s, 1H), 8.44 (d, *J* = 5.6 Hz, 1H) ppm.; ¹³C NMR (75 MHz, CDCl₃) δ 26.2, 61.9, 110.4, 114.5, 114.8, 121.1, 121.4, 122.0, 122.7, 129.6, 134.3, 145.6, 150.0,

152.5, 154.1, 158.1, 164.3, 165.5 ppm.; HRMS (ESI+) *m/z*: calcd. for C₂₂H₁₉N₅O₃Na [M+Na]⁺ 424.1386, found 424.1374.

4-(4-(4-((2-fluorophenoxy)methyl)-1H-1,2,3-triazol-1-yl)phenoxy)-N-methylpicolinamide (2b) [42]

Purification by silica gel column chromatography using 50% EtOAc: *n*-hexane as eluent gave orange-brown solid with 27% yield. ¹H NMR (300 MHz, DMSO-*d*₆) δ 2.78 (d, *J* = 4.9 Hz, 3H), 5.31 (s, 2H), 6.97 (m, 1H), 7.19 (m, 3H), 7.38 (td, *J* = 8.5, 1.1 Hz, 1H), 7.46 (m, 3H), 8.02 (dd, *J* = 6.8, 2.2 Hz, 2H), 8.55 (d, *J* = 5.6 Hz, 1H), 8.82 (q, *J* = 4.9 Hz, 1H), 8.94 (s, 1H) ppm.; ¹³C NMR (75 MHz, DMSO-*d*₆) δ 26.3, 62.1, 109.7, 114.9, 115.9, 116.4 (d, ²*J*_{FC} = 17.3 Hz), 122.0 (d, ³*J*_{FC} = 6.8 Hz), 122.5, 122.9, 123.6, 125.2 (d, ³*J*_{FC} = 3.8 Hz), 134.2, 143.8, 146.0 (d, ²*J*_{FC} = 10.5 Hz), 152.1 (d, ¹*J*_{FC} = 241.5 Hz), 151.0, 152.7, 153.7, 164.1, 165.4 ppm.; ¹⁹F NMR (282 MHz, DMSO-*d*₆) δ -136.7 (s, 1F) ppm.; HRMS (ESI+) *m/z*: calcd. for C₂₂H₁₉FN₅O₃ [M+H]⁺ 420.1472, found 420.1456.

4-(4-(4-((3-fluorophenoxy)methyl)-1H-1,2,3-triazol-1-yl)phenoxy)-N-methylpicolinamide (2c) [42]

Purification by silica gel column chromatography using 50% EtOAc: *n*-hexane as eluent gave white solid with 53% yield. ¹H NMR (300 MHz, DMSO-*d*₆) δ 2.79 (d, *J* = 4.9 Hz, 3H), 5.26 (s, 2H), 6.79 (td, *J* = 8.3, 1.9 Hz, 1H), 6.92 (dd, *J* = 8.2, 2.0 Hz, 1H), 6.98 (dt, *J* = 11.3, 2.3 Hz, 1H), 7.24 (dd, *J* = 5.6, 2.6 Hz, 1H), 7.35 (m, 1H), 7.47 (m, 3H), 8.03 (dd, *J* = 6.9, 2.0 Hz, 2H), 8.56 (d, *J* = 5.6 Hz, 1H), 8.81 (q, *J* = 8.4 Hz, 1H), 8.97 (s, 1H) ppm.; ¹³C NMR (75 MHz, DMSO-*d*₆) δ 26.2, 61.5, 102.5 (d, ²*J*_{FC} = 24.8 Hz), 107.8 (d, ³*J*_{FC} = 21.0 Hz), 109.6, 111.3 (d, ⁴*J*_{FC} = 3.0 Hz), 114.7, 122.4, 122.7, 123.3, 130.9, 131.0, 134.1, 143.7, 150.7, 153.0 (d, ²*J*_{FC} = 68.3 Hz), 159.5 (d, ³*J*_{FC} = 10.5 Hz), 163.1 (d, ¹*J*_{FC} = 241.5 Hz), 163.8, 165.3 ppm.; ¹⁹F NMR (282 MHz, DMSO-*d*₆) δ -113.2 (s, 1F) ppm.; HRMS (ESI+) *m/z*: calcd. for C₂₂H₁₉FN₅O₃Na [M+Na]⁺ 420.1472, found 420.1473.

4-(4-(4-((4-fluorophenoxy)methyl)-1H-1,2,3-triazol-1-yl)phenoxy)-N-methylpicolinamide (2d) [42]

Purification by silica gel column chromatography using 50% EtOAc: *n*-hexane as eluent gave white solid with 35% yield. ¹H NMR (300 MHz, DMSO-*d*₆) δ 2.80 (d, *J* = 4.9 Hz, 3H), 5.24 (s, 2H), 7.13 (m, 4H), 7.26 (dd, *J* = 5.6, 2.6 Hz, 1H), 7.50 (m, 3H), 8.05 (dd, *J* = 6.8, 2.2 Hz, 2H), 8.57 (d, *J* = 5.6 Hz, 1H), 8.82 (q, *J* = 4.8 Hz, 1H), 9.00 (s, 1H) ppm.; ¹³C NMR (75 MHz, DMSO-*d*₆) δ 26.0, 61.6, 109.4, 114.6, 115.9 (d, ²*J*_{FC} = 23.0 Hz), 116.1 (d, ³*J*_{FC} = 8.0 Hz), 121.9, 122.5, 123.1, 134.0, 143.7, 150.6, 152.6, 153.3, 154.3 (d, ⁴*J*_{FC} = 2.3 Hz), 156.7 (d, ¹*J*_{FC} = 234.8 Hz), 163.7, 165.1 ppm.; ¹⁹F NMR (282 MHz, DMSO-*d*₆) δ -125.8 (s, 1F) ppm.; HRMS (ESI+) *m/z*: calcd. for C₂₂H₁₈FN₅O₃Na [M+Na]⁺ 442.1291, found 442.1290.

N-methyl-4-(4-(4-((2-nitrophenoxy)methyl)-1H-1,2,3-triazol-1-yl)phenoxy)picolinamide (2e) [42]

Purification by silica gel column chromatography using 50% EtOAc: *n*-hexane as eluent gave white solid with 38% yield. ¹H NMR (300 MHz, DMSO-*d*₆) δ 2.80 (d, *J* = 4.8 Hz, 3H), 5.46 (s, 2H), 7.16 (t, *J* = 7.5 Hz, 1H), 7.25 (dd, *J* = 5.6, 2.6 Hz, 1H), 7.47 (d, *J* = 8.7 Hz, 3H), 7.63 (d, *J* = 7.8 Hz, 1H), 7.70 (td, *J* = 8.6, 1.4 Hz, 1H), 7.87 (dd, *J* = 8.1, 1.4 Hz, 1H), 8.04 (d, *J* = 8.9 Hz, 2H), 8.56 (d, *J* = 5.6 Hz, 1H), 8.83 (q, *J* = 4.7 Hz, 1H), 8.96 (s, 1H) ppm.; ¹³C NMR (75 MHz, DMSO-*d*₆) δ 26.3, 62.6, 109.8, 114.9, 115.9, 121.5, 122.5, 122.9, 123.7, 125.2, 134.1, 134.7, 140.8, 143.2, 150.7, 150.9, 152.6, 153.7, 164.0, 165.4 ppm.; HRMS (ESI+) *m/z*: calcd. for C₂₂H₁₈N₆O₅ [M+H]⁺ 447.1417, found 477.1413.

N-methyl-4-(4-(4-((3-nitrophenoxy)methyl)-1H-1,2,3-triazol-1-yl)phenoxy)picolinamide (2f) [42]

Purification by silica gel column chromatography using 50% EtOAc: *n*-hexane as eluent gave white solid with 38% yield. ¹H NMR (300 MHz, DMSO-*d*₆) δ 2.79 (d, *J* = 4.8 Hz, 3H), 5.41 (s, 2H), 7.25 (dd, *J* = 5.6, 2.6 Hz, 1H), 7.48 (dd, *J* = 5.4, 2.6 Hz, 3H), 7.59 (m, 2H), 7.86 (d, *J* = 7.8 Hz, 1H), 7.91 (t, *J* = 2.2 Hz, 1H), 8.04 (d, *J* = 8.9 Hz, 2H), 8.56 (d, *J* = 5.6 Hz, 1H), 8.82 (q, *J* = 4.7 Hz, 1H), 8.99 (s, 1H) ppm.; ¹³C NMR (75 MHz, DMSO-*d*₆) δ 26.0, 61.8, 109.3, 109.4, 114.6, 116.0, 122.2, 122.3, 122.6,

123.3, 130.8, 134.0, 143.3, 148.8, 150.6, 152.6, 153.4, 158.5, 163.7, 165.1 ppm.; HRMS (ESI+) m/z : calcd. for $C_{22}H_{18}N_6O_5$ $[M+H]^+$ 447.1417, found 477.1418.

***N*-methyl-4-(4-(4-(4-nitrophenoxy)methyl)-1*H*-1,2,3-triazol-1-yl)phenoxy)picolinamide (2g) [42]**

Purification by silica gel column chromatography using 50% EtOAc: *n*-hexane as eluent gave white solid with 18% yield. 1H NMR (300 MHz, DMSO- d_6) δ 2.80 (d, $J = 4.9$ Hz, 3H), 5.45 (s, 2H), 7.26 (dd, $J = 5.6$, 2.6 Hz, 1H), 7.33 (d, $J = 9.2$ Hz, 2H), 7.50 (m, 3H), 8.06 (d, $J = 8.9$ Hz, 2H), 8.26 (d, $J = 9.2$ Hz, 2H), 8.57 (d, $J = 5.6$ Hz, 1H), 8.81 (q, $J = 4.7$ Hz, 1H), 9.05 (s, 1H) ppm.; ^{13}C NMR (75 MHz, DMSO- d_6) δ 26.0, 61.9, 109.4, 114.6, 115.4, 122.3, 122.6, 123.5, 125.9, 134.0, 141.2, 143.0, 150.6, 152.6, 153.4, 163.2, 163.2, 165.1 ppm.; HRMS (ESI+) m/z : calcd. for $C_{22}H_{18}N_6O_5Na$ $[M+Na]^+$ 469.1236, found 469.1229.

***N*-methyl-4-(4-(4-(2-(trifluoromethyl)phenoxy)methyl)-1*H*-1,2,3-triazol-1-yl)phenoxy)picolinamide (2h)**

Purification by silica gel column chromatography using 50% EtOAc: *n*-hexane as eluent gave white solid with 47% yield. Mp. = 144–145 °C; 1H NMR (300 MHz, DMSO- d_6) δ 2.79 (d, $J = 4.9$ Hz, 3H), 5.42 (s, 2H), 7.14 (t, $J = 7.6$ Hz, 1H), 7.24 (dd, $J = 5.9$, 2.6 Hz, 1H), 7.49 (m, 3H), 7.55 (d, $J = 8.3$ Hz, 1H), 7.66 (q, $J = 7.8$ Hz, 2H), 8.04 (d, $J = 9.0$ Hz, 2H), 8.56 (d, $J = 5.6$ Hz, 1H), 8.80 (q, $J = 4.9$ Hz, 1H), 8.97 (s, 1H) ppm.; ^{13}C NMR (75 MHz, DMSO- d_6) δ 26.0, 61.9, 109.4, 114.3, 114.6, 117.4 (q, $^2J_{FC} = 30.6$ Hz), 123.7 (q, $^1J_{FC} = 270.6$ Hz), 120.8, 122.3, 122.6, 123.2, 126.8 (q, $^3J_{FC} = 5.3$ Hz), 133.9, 134.2, 143.3, 150.6, 152.6, 153.4, 156.8, 163.7, 165.1 ppm.; ^{19}F NMR (282 MHz, DMSO- d_6) δ -62.6 (s, 3F) ppm.; HRMS (ESI+) m/z : calcd for $C_{23}H_{19}F_3N_5O_3$ $[M+H]^+$ 470.1440, found 470.1439.

***N*-methyl-4-(4-(4-(3-(trifluoromethyl)phenoxy)methyl)-1*H*-1,2,3-triazol-1-yl)phenoxy)picolinamide (2i)**

Purification by silica gel column chromatography using 50% EtOAc: *n*-hexane as eluent gave white solid with 53% yield. Mp. = 147–148 °C; 1H NMR (300 MHz, DMSO- d_6) δ 2.79 (d, $J = 4.9$ Hz, 3H), 5.36 (s, 2H), 7.26 (dd, $J = 5.6$, 2.6 Hz, 2H), 7.33 (d, $J = 7.8$ Hz, 1H), 7.40 (br s, 1H), 7.42 (s, 1H), 7.49 (m, 3H), 7.56 (t, $J = 8.6$ Hz, 1H), 8.04 (d, $J = 9.0$ Hz, 2H), 8.56 (d, $J = 5.6$ Hz, 1H), 8.81 (q, $J = 4.9$ Hz, 1H), 9.01 (s, 1H) ppm.; ^{13}C NMR (75 MHz, DMSO- d_6) δ 26.1, 61.5, 109.4, 111.5 (q, $^3J_{FC} = 3.8$ Hz), 114.6, 117.6 (q, $^3J_{FC} = 3.8$ Hz), 124.0 (q, $^1J_{FC} = 270.8$ Hz), 119.1, 122.3, 122.6, 123.3, 130.4 (q, $^2J_{FC} = 31.5$ Hz), 130.8, 134.0, 143.6, 150.6, 152.3, 153.4, 158.3, 163.7, 165.2 ppm.; ^{19}F NMR (282 MHz, DMSO- d_6) δ -62.6 (s, 3F) ppm.; HRMS (ESI+) m/z : calcd for $C_{23}H_{19}F_3N_5O_3$ $[M+H]^+$ 470.1440, found 470.1437.

***N*-methyl-4-(4-(4-(4-(trifluoromethyl)phenoxy)methyl)-1*H*-1,2,3-triazol-1-yl)phenoxy)picolinamide (2j)**

Purification by silica gel column chromatography using 50% EtOAc: *n*-hexane as eluent gave white solid with 42% yield. Mp. = 173–173 °C; 1H NMR (300 MHz, DMSO- d_6) δ 2.80 (d, $J = 4.9$ Hz, 3H), 5.37 (s, 2H), 7.28 (m, 3H), 7.49 (m, 3H), 7.69 (d, $J = 8.6$ Hz, 2H), 8.05 (dd, $J = 9.0$ Hz, 2H), 8.56 (d, $J = 5.6$ Hz, 1H), 8.82 (q, $J = 4.5$ Hz, 1H), 9.02 (s, 1H) ppm.; ^{13}C NMR (75 MHz, DMSO- d_6) δ 26.0, 61.3, 109.4, 114.6, 115.3, 124.5 (q, $^1J_{FC} = 269.3$ Hz), 121.6 (q, $^2J_{FC} = 31.9$ Hz), 122.2, 122.6, 123.3, 126.0 (q, $^3J_{FC} = 3.8$ Hz), 134.0, 143.4, 150.6, 152.6, 153.4, 160.8, 163.6, 165.1 ppm.; ^{19}F NMR (282 MHz, DMSO- d_6) δ -61.5 (s, 3F) ppm.; HRMS (ESI+) m/z : calcd for $C_{23}H_{19}FN_5O_3$ $[M+H]^+$ 470.1440, found 470.1431.

4-(4-(4-(2-(*tert*-butyl)phenoxy)methyl)-1*H*-1,2,3-triazol-1-yl)phenoxy)-*N*-methylpicolinamide (2k)

Purification by silica gel column chromatography using 30% EtOAc: *n*-hexane as eluent gave white solid with 42% yield. Mp. = 139–140 °C; 1H NMR (300 MHz, DMSO- d_6) δ 1.30 (s, 9H), 2.79 (d, $J = 4.8$ Hz, 3H), 5.25 (s, 2H), 6.90 (m, 1H), 7.22 (m, 4H), 7.47 (m, 3H), 8.05 (d, $J = 8.9$ Hz, 2H), 8.56 (d, $J = 5.6$ Hz, 1H), 8.81 (q, $J = 4.7$ Hz, 1H), 8.94 (s, 1H) ppm.; ^{13}C NMR (75 MHz, DMSO- d_6) δ 24.5, 29.9, 34.6, 61.2, 109.71, 113.2, 114.8, 121.0, 122.5, 122.7, 123.0, 126.6, 127.4, 134.2, 137.8, 144.4, 150.8, 152.6, 153.6, 157.0, 164.0, 165.4 ppm.; HRMS (ESI+) m/z : calcd for $C_{26}H_{27}N_5O_3Na$ $[M+Na]^+$ 480.2012, found 480.2017.

4-(4-(4-(3-(*tert*-butyl)phenoxy)methyl)-1*H*-1,2,3-triazol-1-yl)phenoxy)-*N*-methylpicolinamide (2l)

Purification by silica gel column chromatography using 30% EtOAc: *n*-hexane as eluent gave white solid with 31% yield. Mp. = 119–121 °C; 1H NMR (300 MHz, DMSO- d_6) δ 1.25 (s, 9H), 2.79 (d, $J = 4.9$ Hz, 3H), 5.23 (s, 2H), 6.91 (d, $J = 7.7$, 1.9 Hz, 1H), 7.00 (m, 2H), 7.24 (m, 2H), 7.45 (s, 1H), 7.47 (d, $J = 3.0$ Hz, 2H), 8.03 (dd, $J = 6.9$, 2.0 Hz, 2H), 8.6 (d, $J = 5.6$ Hz, 1H), 8.81 (q, $J = 8.4$ Hz, 1H), 8.94 (s, 1H) ppm.; ^{13}C NMR (75 MHz, DMSO- d_6) δ 26.2, 31.2, 34.6, 61.0, 109.6, 111.3, 112.6, 114.8, 118.1, 122.4, 122.7, 123.2, 129.3, 134.2, 144.4, 150.8, 152.6, 152.7, 153.5, 158.0, 163.9, 165.4 ppm.; HRMS (ESI+) m/z : calcd for $C_{26}H_{28}N_5O_3$ $[M+H]^+$ 458.2192, found 458.2199.

4-(4-(4-(4-(*tert*-butyl)phenoxy)methyl)-1*H*-1,2,3-triazol-1-yl)phenoxy)-*N*-methylpicolinamide (2m)

Purification by silica gel column chromatography using 50% EtOAc: *n*-hexane as eluent gave white solid with 44% yield. Mp. = 157–159 °C; 1H NMR (300 MHz, DMSO- d_6) δ 1.25 (s, 9H), 2.79 (d, $J = 4.9$ Hz, 3H), 5.22 (s, 2H), 6.99 (d, $J = 8.9$ Hz, 2H), 7.24 (dd, $J = 5.6$, 2.6 Hz, 1H), 7.32 (d, $J = 8.9$ Hz, 2H), 7.48 (d, $J = 9.0$ Hz, 2H), 7.48 (d, $J = 2.4$ Hz, 1H), 8.05 (d, $J = 9.0$ Hz, 2H), 8.56 (d, $J = 5.6$ Hz, 1H), 8.81 (q, $J = 4.9$ Hz, 1H), 8.98 (s, 1H) ppm.; ^{13}C NMR (75 MHz, DMSO- d_6) δ 26.0, 31.3, 33.8, 61.0, 109.4, 114.0, 114.6, 122.2, 122.5, 122.9, 126.1, 134.0, 143.1, 144.2, 150.6, 152.6, 153.3, 155.8, 163.7, 165.1 ppm.; HRMS (ESI+) m/z : calcd for $C_{26}H_{28}N_5O_3$ $[M+H]^+$ 458.2192, found 458.2196.

4-(4-(4-(2,3-difluorophenoxy)methyl)-1*H*-1,2,3-triazol-1-yl)phenoxy)-*N*-methylpicolinamide (2n)

Purification by silica gel column chromatography using 30% EtOAc: *n*-hexane as eluent gave white solid with 18% yield. Mp. = 146–148 °C; 1H NMR (300 MHz, DMSO- d_6) δ 2.78 (d, $J = 4.8$ Hz, 3H), 5.39 (s, 2H), 7.04 (dd, $J = 17.0$, 8.5 Hz, 1H), 7.23 (m, 3H), 7.49 (m, 3H), 8.06 (d, $J = 8.8$ Hz, 2H), 8.56 (d, $J = 5.6$ Hz, 1H), 8.80 (q, $J = 4.7$ Hz, 1H), 9.03 (s, 1H) ppm.; ^{13}C NMR (75 MHz, DMSO- d_6) δ 26.0, 62.4, 109.4 (d, $^3J_{FC} = 5.3$ Hz), 109.6, 111.1, 114.6, 122.2, 122.6, 123.5, 124.2 (dd, $^2J_{FC}$, $^3J_{FC} = 9.0$, 5.3 Hz), 134.0, 140.3 (dd, $^1J_{FC}$, $^2J_{FC} = 243.8$, 15.0 Hz), 143.1, 147.4 (d, $^3J_{FC} = 4.5$ Hz), 150.5 (dd, $^1J_{FC}$, $^2J_{FC} = 243.0$, 10.5 Hz), 150.6, 152.6, 153.4, 163.7, 165.1 ppm.; ^{19}F NMR (282 MHz, DMSO- d_6) δ -140.2 (s, 1F), -140.3 (s, 1F) ppm.; HRMS (ESI+) m/z : calcd for $C_{22}H_{17}F_2N_5O_3Na$ $[M+Na]^+$ 460.1197, found 460.1195.

4-(4-(4-(2,4-difluorophenoxy)methyl)-1*H*-1,2,3-triazol-1-yl)phenoxy)-*N*-methylpicolinamide (2o)

Purification by silica gel column chromatography using 30% EtOAc: *n*-hexane as eluent gave white solid with 31% yield. Mp. = 179–180 °C; 1H NMR (300 MHz, DMSO- d_6) δ 2.79 (d, $J = 4.8$ Hz, 3H), 5.30 (s, 2H), 7.14 (m, 1H), 7.27 (m, 2H), 7.40 (m, 1H), 7.47 (m, 3H), 8.03 (d, $J = 8.9$ Hz, 2H), 8.80 (d, $J = 5.6$ Hz, 1H), 8.80 (q, $J = 4.7$ Hz, 1H), 8.95 (s, 1H) ppm.; ^{13}C NMR (75 MHz, DMSO- d_6) δ 26.2, 62.7, 105.0 (dd, $^2J_{FC} = 27.0$, 21.8 Hz), 109.6, 111.1 (dd, $^2J_{FC}$, $^4J_{FC} = 22.5$, 3.8 Hz), 114.8, 116.8 (d, $^3J_{FC} = 9.0$ Hz), 122.4, 123.5, 134.1, 142.6 (dd, $^2J_{FC}$, $^4J_{FC} = 10.5$, 3.0 Hz), 143.5, 152.3 (dd, $^1J_{FC}$, $^3J_{FC} = 245.3$, 12.8 Hz), 150.8, 152.6, 153.5, 156.1 (d, $^1J_{FC}$, $^3J_{FC} = 238.5$, 10.5 Hz), 157.7 (d, $^2J_{FC} = 36.5$ Hz) 164.0, 165.3 ppm.; ^{19}F NMR (282 MHz, DMSO- d_6) δ -121.4 (d, $J_{FF} = 2.7$ Hz, 1F), -131.3 (d, $J_{FF} = 2.7$ Hz, 1F) ppm.; HRMS (ESI+) m/z : calcd for $C_{22}H_{18}F_2N_5O_3$ $[M+H]^+$ 438.1378, found 438.1376.

4-(4-(4-(2,5-difluorophenoxy)methyl)-1*H*-1,2,3-triazol-1-yl)phenoxy)-*N*-methylpicolinamide (2p)

Purification by silica gel column chromatography using 30% EtOAc: *n*-hexane as eluent gave white solid with 51% yield. Mp. = 184–185 °C; 1H NMR (300 MHz, DMSO- d_6) δ 2.79 (d, $J = 4.8$ Hz, 3H), 5.36 (s, 2H), 6.81 (tt, $J = 8.5$, 3.1 Hz, 1H), 7.25 (dd, $J = 5.7$, 2.7 Hz, 1H), 7.29 (m, 1H), 7.39 (m, 1H), 7.49 (m, 2H), 8.06 (d, $J = 8.9$ Hz, 2H), 8.56 (d, $J = 5.6$ Hz, 1H), 8.80 (q, $J = 4.7$ Hz, 1H), 9.03 (s, 1H) ppm.; ^{13}C NMR (75 MHz, DMSO- d_6) δ 26.0, 62.2, 103.5 (d, $^2J_{FC} = 27.8$ Hz), 107.0 (dd, $^2J_{FC}$, $^3J_{FC} = 23.3$, 6.8 Hz), 109.4, 114.6, 116.5 (dd, $^2J_{FC}$, $^3J_{FC} = 20.3$, 19.5 Hz), 122.2, 122.6, 123.5, 134.0, 143.0, 148.2 (dd, $^1J_{FC}$, $^4J_{FC} = 238.5$, 2.8 Hz), 150.7, 152.6, 153.4, 158.2 (dd, $^1J_{FC}$, $^4J_{FC} = 236.3$, 2.6 Hz), 163.0, 163.7, 165.1 ppm.; ^{19}F NMR (282 MHz, DMSO- d_6) δ -117.9 (d, $J_{FF} = 15.3$ Hz,

1F), -141.6 (d, $J_{FF} = 15.3$ Hz, 1F) ppm.; HRMS (ESI+) m/z : calcd for $C_{22}H_{17}F_2N_5O_3Na$ $[M+Na]^+$ 460.1197, found 460.1194.

4-(4-(4-((2,6-difluorophenoxy)methyl)-1H-1,2,3-triazol-1-yl)phenoxy)-N-methylpicolinamide (2q)

Purification by silica gel column chromatography using 30% EtOAc: *n*-hexane as eluent gave white solid with 61% yield. Mp. = 167–169 °C; 1H NMR (75 MHz, DMSO- d_6) δ 2.80 (d, $J = 4.9$ Hz, 3H), 5.30 (s, 2H), 7.16 (m, 3H), 7.25 (dd, $J = 5.6, 2.6$ Hz, 1H), 7.48 (m, 3H), 8.04 (d, $J = 8.9$ Hz, 2H), 8.56 (d, $J = 5.6$ Hz, 1H), 8.80 (q, $J = 4.8$ Hz, 1H), 9.00 (s, 1H) ppm.; ^{13}C NMR (75 MHz, DMSO- d_6) δ 26.0, 66.4 (t, $^4J_{FC} = 2.9$ Hz), 109.9, 112.6 (d, $^2J_{FC} = 22.5$ Hz), 112.5 (d, $^3J_{FC} = 9.0$ Hz), 114.6, 122.3, 122.4, 123.4, 124.3 (t, $^3J_{FC} = 9.4$ Hz), 133.9, 143.3, 150.6, 153.0 (d, $^2J_{FC} = 55.8$ Hz), 154.1 (d, $^2J_{FC} = 5.4$ Hz) 155.7 (dd, $^1J_{FC}, ^3J_{FC} = 245.3, 5.3$ Hz), 163.7, 165.1 ppm.; ^{19}F NMR (282 MHz, DMSO- d_6) δ -130.1 (s, 2F) ppm.; HRMS (ESI+) m/z : calcd for $C_{22}H_{17}F_2N_5O_3Na$ $[M+Na]^+$ 460.1197, found 460.1199.

4-(4-(4-((3,4-difluorophenoxy)methyl)-1H-1,2,3-triazol-1-yl)phenoxy)-N-methylpicolinamide (2r)

Purification by silica gel column chromatography using 50% EtOAc: *n*-hexane as eluent gave white solid with 31% yield. Mp. = 179–181 °C; 1H NMR (300 MHz, DMSO- d_6) δ 2.80 (d, $J = 4.8$ Hz, 3H), 5.26 (s, 2H), 6.93 (m, 1H), 7.25 (dd, $J = 19.4, 3.1$ Hz, 1H), 7.26 (dd, $J = 5.6, 2.6$ Hz, 1H), 7.39 (dd, $J = 19.7, 9.5$ Hz, 1H), 7.49 (d, $J = 8.9$ Hz, 2H), 7.50 (d, $J = 2.9$ Hz, 1H), 8.05 (d, $J = 8.9$ Hz, 2H), 8.57 (d, $J = 5.6$ Hz, 1H), 8.80 (q, $J = 4.8$ Hz, 1H), 8.99 (s, 1H) ppm.; ^{13}C NMR (75 MHz, DMSO- d_6) δ 26.0, 61.9, 104.5 (d, $^2J_{FC} = 20.3$ Hz), 109.4, 111.2 (dd, $^3J_{FC}, ^4J_{FC} = 5.3, 3.0$ Hz), 114.6, 117.6 (d, $^2J_{FC} = 18.0$ Hz), 122.2, 122.6, 123.3, 134.0, 144.2 (dd, $^1J_{FC}, ^2J_{FC} = 236.3, 12.8$ Hz), 143.4, 149.6 (dd, $^1J_{FC}, ^2J_{FC} = 243.0, 13.5$ Hz), 150.6, 152.6, 153.4, 154.6 (d, $^3J_{FC} = 9.0$ Hz), 163.7, 165.1 ppm.; ^{19}F NMR (282 MHz, DMSO- d_6) δ -164.0 (d, $J_{FF} = 22.6$ Hz, 1F) ppm.; HRMS (ESI+) m/z : calcd for $C_{22}H_{18}F_2N_5O_3$ $[M+H]^+$ 438.1378, found 438.1379.

4-(4-(4-((3,5-difluorophenoxy)methyl)-1H-1,2,3-triazol-1-yl)phenoxy)-N-methylpicolinamide (2s)

Purification by silica gel column chromatography using 30% EtOAc: *n*-hexane as eluent gave white solid with 42% yield. Mp. = 199–201 °C; 1H NMR (300 MHz, DMSO- d_6) δ 2.79 (d, $J = 4.9$ Hz, 3H), 5.28 (s, 2H), 6.84 (m, 3H), 7.25 (dd, $J = 5.6, 2.9$ Hz, 1H), 7.48 (m, 3H), 8.03 (d, $J = 8.9$ Hz, 2H), 8.56 (d, $J = 5.6$ Hz, 1H), 8.82 (q, $J = 4.9$ Hz, 1H), 8.98 (s, 1H) ppm.; ^{13}C NMR (75 MHz, DMSO- d_6) δ 26.2, 61.9, 96.7 (t, $^2J_{FC} = 26.3$ Hz), 99.2 (d, $^2J_{FC} = 28.5$ Hz), 109.6, 114.8, 122.4, 122.8, 123.6, 134.1, 143.3, 150.8, 152.6, 153.6, 160.2 (t, $^3J_{FC} = 14.3$ Hz), 163.2 (dd, $^1J_{FC}, ^3J_{FC} = 242.3, 15.8$ Hz), 163.9, 165.3 ppm.; ^{19}F NMR (282 MHz, DMSO- d_6) δ -110.7 (s, 2F) ppm.; HRMS (ESI+) m/z : calcd for $C_{22}H_{17}F_2N_5O_3Na$ $[M+Na]^+$ 460.1197, found 460.1196.

4-(4-(4-((3,5-bis(trifluoromethyl)phenoxy)methyl)-1H-1,2,3-triazol-1-yl)phenoxy)-N-methylpicolinamide (2t)

Purification by silica gel column chromatography using 50% EtOAc: *n*-hexane as eluent gave white solid with 62% yield. Mp. = 174–175 °C; 1H NMR (300 MHz, DMSO- d_6) δ 2.80 (d, $J = 4.9$ Hz, 3H), 5.50 (s, 2H), 7.26 (dd, $J = 5.6, 2.6$ Hz, 1H), 7.50 (dd, $J = 6.1, 3.3$ Hz, 3H), 7.68 (s, 1H), 7.80 (s, 2H), 8.05 (d, $J = 8.9$ Hz, 2H), 8.57 (d, $J = 5.6$ Hz, 1H), 8.81 (q, $J = 4.8$ Hz, 1H), 9.03 (s, 1H) ppm.; ^{13}C NMR (75 MHz, DMSO- d_6) δ 26.1, 62.1, 109.5, 114.2 (m), 114.7, 116.1, 123.2 (q, $^1J_{FC} = 271.2$ Hz), 122.3, 122.6, 123.5, 131.6 (q, $^2J_{FC} = 32.8$ Hz), 134.0, 143.1, 150.6, 152.6, 153.5, 159.0, 163.7, 165.2 ppm.; ^{19}F NMR (282 MHz, DMSO- d_6) δ -63.0 (s, 6F) ppm.; HRMS (ESI+) m/z : calcd for $C_{24}H_{18}F_6N_5O_3$ $[M+H]^+$ 538.1314, found 538.1301.

4-(4-(4-((4-chloro-3-(trifluoromethyl)phenoxy)methyl)-1H-1,2,3-triazol-1-yl)phenoxy)-N-methylpicolinamide (2u)

Purification by silica gel column chromatography using 50% EtOAc: *n*-hexane as eluent gave pale-pink solid with 36% yield. Mp. = 172–174 °C; 1H NMR (300 MHz, DMSO- d_6) δ 2.79 (d, $J = 4.9$ Hz, 3H), 5.38 (s, 2H), 7.26 (dd, $J = 5.6, 2.6$ Hz, 1H), 7.44 (dd, $J = 9.0, 3.0$ Hz, 1H), 7.50 (m, 4H), 7.67 (d, $J = 8.9$ Hz, 1H), 8.04 (d, $J = 9.0$ Hz, 2H), 8.56 (d, $J = 5.6$ Hz, 1H), 8.81 (q, $J = 4.9$ Hz, 1H), 9.00 (s, 1H) ppm.; ^{13}C

NMR (75 MHz, DMSO- d_6) δ 26.1, 61.8, 109.4, 120.6 (q, $^1J_{FC} = 266.8$ Hz), 114.7, 120.3, 122.0, 122.3, 122.6, 123.4, 127.3, 132.8, 134.0, 143.3, 150.6, 152.5, 153.4, 156.8, 158.3 (q, $^2J_{FC} = 37.0$ Hz), 163.7, 165.2 ppm.; ^{19}F NMR (282 MHz, DMSO- d_6) δ -63.0 (s, 3F) ppm.; HRMS (ESI+) m/z : calcd for $C_{23}H_{18}ClF_3N_5O_3$ $[M+H]^+$ 504.1050, found 504.1045.

N-methyl-4-(4-(4-(*p*-toloxy)methyl)-1H-1,2,3-triazol-1-yl)phenoxy)picolinamide (2v)

Purification by silica gel column chromatography using 50% EtOAc: *n*-hexane as eluent gave white solid with 77% yield. Mp. = 152–154 °C; 1H NMR (300 MHz, DMSO- d_6) δ 2.24 (s, 3H), 2.80 (d, $J = 9.0$ Hz, 2H), 5.20 (s, 2H), 6.97 (d, $J = 9.0$ Hz, 2H), 7.12 (d, $J = 9.0$ Hz, 2H), 7.24 (dd, $J = 5.6, 2.6$ Hz, 1H), 7.49 (m, 3H), 8.05 (d, $J = 8.9$ Hz, 2H), 8.56 (d, $J = 5.6$ Hz, 1H), 8.80 (q, $J = 7.7, 4.9$ Hz, 1H), 8.97 (s, 1H) ppm.; ^{13}C NMR (75 MHz, DMSO- d_6) δ 20.1, 26.0, 61.0, 109.4, 114.6, 114.6, 122.2, 122.5, 123.0, 129.7, 129.9, 134.0, 144.1, 150.6, 152.6, 153.3, 155.9, 163.6, 165.2 ppm.; HRMS (ESI+) m/z : calcd for $C_{23}H_{22}N_5O_3$ $[M+H]^+$ 416.1723, found 416.1717.

4-(4-(4-((4-ethylphenoxy)methyl)-1H-1,2,3-triazol-1-yl)phenoxy)-N-methylpicolinamide (2w)

Purification by silica gel column chromatography using 30% EtOAc: *n*-hexane as eluent gave light-yellow solid with 39% yield. Mp. = 143–145 °C; 1H NMR (300 MHz, DMSO- d_6) δ 1.14 (t, $J = 7.6$ Hz, 3H), 2.54 (q, $J = 7.6$ Hz, 2H), 2.79 (d, $J = 4.8$ Hz, 3H), 5.21 (s, 2H), 6.99 (d, $J = 8.6$ Hz, 2H), 7.14 (d, $J = 8.6$ Hz, 2H), 7.25 (dd, $J = 5.6, 2.6$ Hz, 1H), 7.28 (dd, $J = 7.1, 2.0$ Hz, 3H), 8.04 (d, $J = 8.9$ Hz, 2H), 8.56 (d, $J = 5.6$ Hz, 1H), 8.81 (dq, $J = 5.1$ Hz, 1H), 8.97 (s, 1H) ppm.; ^{13}C NMR (75 MHz, DMSO- d_6) δ 15.9, 26.1, 27.3, 61.1, 109.4, 114.6, 114.7, 122.3, 122.5, 123.0, 128.7, 134.1, 136.2, 144.2, 150.6, 152.5, 153.3, 156.1, 163.7, 165.2 ppm.; HRMS (ESI+) m/z : calcd for $C_{24}H_{23}N_5O_3Na$ $[M+Na]^+$ 452.1699, found 452.1691.

4-(4-(4-((4-isopropylphenoxy)methyl)-1H-1,2,3-triazol-1-yl)phenoxy)-N-methylpicolinamide (2x)

Purification by silica gel column chromatography using 30% EtOAc: *n*-hexane as eluent gave white solid with 44% yield. Mp. = 140–142 °C; 1H NMR (300 MHz, DMSO- d_6) δ 1.16 (d, $J = 6.9$ Hz, 6H), 2.79 (d, $J = 4.6$ Hz, 3H), 2.85 (m, 1H), 5.20 (s, 2H), 6.98 (d, $J = 8.7$ Hz, 2H), 7.17 (d, $J = 8.6$ Hz, 2H), 7.24 (dd, $J = 5.6, 2.6$ Hz, 1H), 7.47 (m, 3H), 8.03 (d, $J = 9.0$ Hz, 2H), 8.56 (d, $J = 5.6$ Hz, 1H), 8.81 (q, $J = 4.8$ Hz, 1H), 8.94 (s, 1H) ppm.; ^{13}C NMR (75 MHz, DMSO- d_6) δ 24.2, 26.2, 32.7, 61.1, 109.6, 114.7, 114.8, 122.4, 122.7, 123.1, 127.4, 134.2, 141.2, 144.4, 150.8, 152.6, 153.5, 156.2, 163.9, 165.4 ppm.; HRMS (ESI+) m/z : calcd for $C_{25}H_{26}N_5O_3$ $[M+H]^+$ 444.2036, found 444.2034.

4-(4-(4-((4-chlorophenoxy)methyl)-1H-1,2,3-triazol-1-yl)phenoxy)-N-methylpicolinamide (2y)

Purification by silica gel column chromatography using 50% EtOAc: *n*-hexane as eluent gave white solid with 97% yield. Mp. = 215–217 °C; 1H NMR (300 MHz, DMSO- d_6) δ 2.79 (d, $J = 4.9$ Hz, 3H), 5.26 (s, 2H), 7.13 (d, $J = 9.0$ Hz, 2H), 7.25 (dd, $J = 5.6, 2.6$ Hz, 1H), 7.36 (d, $J = 9.0$ Hz, 2H), 7.48 (d, $J = 8.9$ Hz, 2H), 8.04 (d, $J = 8.9$ Hz, 2H), 8.80 (q, $J = 4.9$ Hz, 1H), 8.99 (s, 1H) ppm.; ^{13}C NMR (75 MHz, DMSO- d_6) δ 26.1, 61.3, 109.5, 114.7, 116.7, 122.4, 122.7, 123.3, 124.8, 129.4, 134.1, 143.8, 150.7, 154.6, 153.5, 156.9, 163.8, 166.2 ppm.; HRMS (ESI+) m/z : calcd for $C_{22}H_{18}ClN_5O_3Na$ $[M+Na]^+$ 458.0996, found 458.0989.

4-(4-(4-((4-bromophenoxy)methyl)-1H-1,2,3-triazol-1-yl)phenoxy)-N-methylpicolinamide (2z)

Purification by silica gel column chromatography using 50% EtOAc: *n*-hexane as eluent gave white solid with 47% yield. Mp. = 217–218 °C; 1H NMR (300 MHz, CDCl₃) δ 3.02 (s, 3H), 5.28 (s, 2H), 6.93 (d, $J = 9.0$ Hz, 2H), 7.06 (dd, $J = 5.6, 2.6$ Hz, 1H), 7.29 (d, $J = 9.0$ Hz, 2H), 7.34 (s, 1H), 7.42 (d, $J = 9.1$ Hz, 2H), 7.73 (d, $J = 2.5$ Hz, 1H), 7.84 (d, $J = 9.0$ Hz, 2H), 8.17 (s, 1H), 8.46 (d, $J = 5.6$ Hz, 1H) ppm.; ^{13}C NMR (75 MHz, CDCl₃) δ 26.1, 62.7, 110.7, 113.8, 114.8, 116.8, 121.6, 122.1, 123.0, 132.6, 134.3, 144.8, 150.3, 152.4, 154.3, 157.3, 164.8, 165.7 ppm.; HRMS (ESI+) m/z : calcd for $C_{22}H_{19}BrN_5O_3$ $[M+H]^+$ 480.0671, 482.0651, found 480.0652, 482.0664.

4-(4-(4-(4-hydroxyphenoxy)methyl)-1H-1,2,3-triazol-1-yl)phenoxy)-N-methylpicolinamide (2aa)

Purification by silica gel column chromatography using 50% EtOAc: *n*-hexane as eluent gave white solid with 31% yield. Mp. = 213–214 °C; ¹H NMR (300 MHz, DMSO-*d*₆) δ 2.78 (d, *J* = 4.8 Hz, 3H), 5.25 (s, 2H), 6.94 (d, *J* = 8.9 Hz, 2H), 7.13 (dd, *J* = 5.6, 2.6 Hz, 1H), 7.36 (d, *J* = 2.5 Hz, 1H), 7.68 (d, *J* = 8.9 Hz, 2H), 8.49 (d, *J* = 5.6 Hz, 1H), 8.77 (m, 2H), 9.97 (br s, 1H) ppm.; ¹³C NMR (75 MHz, DMSO-*d*₆) δ 26.0, 61.5, 108.6, 113.9, 116.1, 116.4, 122.0, 122.3, 122.9, 128.7, 143.4, 146.8, 150.4, 152.4, 155.8, 157.9, 163.8, 166.2 ppm.; HRMS (ESI+) *m/z*: calcd for C₂₂H₁₉N₅O₄Na [M+Na]⁺ 440.1335, found 440.1338.

4-(4-(4-(4-methoxyphenoxy)methyl)-1H-1,2,3-triazol-1-yl)phenoxy)-N-methylpicolinamide (2ab)

Purification by silica gel column chromatography using 50% EtOAc: *n*-hexane as eluent gave white solid with 62% yield. Mp. = 181–183 °C; ¹H NMR (300 MHz, DMSO-*d*₆) δ 2.79 (d, *J* = 4.9 Hz, 3H), 3.69 (s, 3H), 5.17 (s, 2H), 6.86 (d, *J* = 9.2 Hz, 2H), 7.00 (d, *J* = 9.2 Hz, 2H), 7.24 (dd, *J* = 5.6, 2.6 Hz, 1H), 7.47 (m, 3H), 8.03 (d, *J* = 9.0 Hz, 2H), 8.56 (d, *J* = 5.6 Hz, 1H), 8.82 (dq, *J* = 4.9 Hz, 1H), 8.93 (s, 1H) ppm.; ¹³C NMR (75 MHz, DMSO-*d*₆) δ 26.2, 55.5, 61.7, 109.6, 114.8, 114.8, 116.0, 122.4, 122.7, 123.1, 134.2, 144.4, 150.8, 152.1, 152.6, 153.5, 153.8, 163.9, 165.3 ppm.; HRMS (ESI+) *m/z*: calcd for C₂₃H₂₂N₅O₄ [M+H]⁺ 432.1672, found 432.1673.

4-(4-(4-(4-acetamidophenoxy)methyl)-1H-1,2,3-triazol-1-yl)phenoxy)-N-methylpicolinamide (2ac)

Purification by silica gel column chromatography using 50% EtOAc: *n*-hexane as eluent gave white solid with 42% yield. Mp. = 221–222 °C; ¹H NMR (300 MHz, DMSO-*d*₆) δ 2.00 (s, 3H), 2.79 (d, *J* = 4.8 Hz, 3H), 5.19 (s, 2H), 7.00 (d, *J* = 8.9 Hz, 2H), 7.24 (dd, *J* = 5.6, 2.6 Hz, 1H), 7.48 (m, 5H), 8.03 (d, *J* = 8.9 Hz, 2H), 8.55 (d, *J* = 5.6 Hz, 1H), 8.82 (q, *J* = 4.8 Hz, 1H), 8.94 (s, 1H), 9.84 (s, 1H) ppm.; ¹³C NMR (75 MHz, DMSO-*d*₆) δ 23.8, 26.0, 61.2, 109.4, 114.6, 114.8, 120.5, 122.2, 122.5, 123.0, 133.0, 134.0, 144.1, 150.6, 152.6, 153.3, 153.7, 163.6, 165.1, 167.8 ppm.; HRMS (ESI+) *m/z*: calcd for C₂₄H₂₂N₆O₄Na [M+Na]⁺ 481.1600, found 481.1617.

4-(4-(4-(4-aminophenoxy)methyl)-1H-1,2,3-triazol-1-yl)phenoxy)-N-methylpicolinamide (2ad)

To a stirred solution of *N*-methyl-4-(4-(4-(4-nitrophenoxy)methyl)-1H-1,2,3-triazol-1-yl)phenoxy)picolinamide (**2g**) (210 mg, 0.47 mmol) in THF and MeOH (1.7:0.6 mL) was added NaBH₄ (213 mg, 5.63 mmol) and NiCl₂·5H₂O (17.7 mg, 0.075 mmol) at –5 °C, respectively. The reaction mixture was stirred for 2 h and filtered to remove the catalyst. The filtrate was partitioned with water (20 mL) and EtOAc (20 mL) followed by extracted with EtOAc (3x20 mL). The combined organic layer was dried over anhydrous Na₂SO₄, filtered and concentrated under reduced pressure to provide crude product, which was purified by silica gel column chromatography (70% EtOAc: *n*-hexane) to provide **2ad** (151 mg, 0.36 mmol, 77%) as a brown solid. Mp. = 177–179 °C; ¹H NMR (300 MHz, DMSO-*d*₆) δ 2.80 (d, *J* = 4.9 Hz, 3H), 5.17 (s, 2H), 6.87 (d, *J* = 8.9 Hz, 2H), 6.97 (d, *J* = 9.0 Hz, 2H), 7.27 (dd, *J* = 5.6, 2.6 Hz, 1H), 7.50 (m, 3H), 8.05 (d, *J* = 9.0 Hz, 2H), 8.57 (d, *J* = 5.8 Hz, 1H), 8.82 (q, *J* = 5.0 Hz, 1H), 8.97 (s, 1H) ppm.; ¹³C NMR (75 MHz, DMSO-*d*₆) δ 26.1, 61.6, 109.4, 114.7, 115.9, 119.1, 122.3, 122.5, 123.0, 134.1, 134.9, 144.2, 150.7, 152.7, 152.9, 153.4, 163.8, 165.2 ppm.; HRMS (ESI+) *m/z*: calcd for C₂₂H₂₁N₆O₃ [M+H]⁺ 417.1675, found 417.1664.

4.4. In vitro cytotoxicity towards HepG2, Huh7 and MRC-5

The assay of cytotoxic activities against human HCC cell lines, HepG2 and Huh7, were performed using MTT method according to the procedure described by Nagel *et al.* and Zhang *et al.* [47,48]. The cytotoxic activity against normal human lung fibroblast (MRC-5) was evaluated by means of MTT assay as previously described [51]. Sorafenib was used as the reference drug. All experiments were carried out three times with three replicates for each concentration tested. Where applicable, IC₅₀ values were calculated by linear regression (IC₅₀ > 50 µg/mL

(≈ 100 µM) assumes no cytotoxic effects).

4.5. Inhibitory activity assay towards B-RAF [71]

Huh7 cell lines (6.5 × 10⁵ cells/well) were seeded overnight in 12-well plates and treated with the indicated compound concentrations for 24 h at 37 °C under 5% CO₂. The cell lysate was performed immediately and transferred to B-RAF ELISA Kit (Aviva Systems Biology Corporation, San Diego, USA). Assays were performed according to the manufacturer's instruction. Then the concentration of B-RAF was determined by measuring the absorbance at 450 nm. The B-RAF concentration contained in the samples can be interpolated by using linear regression of each mean sample Relative OD450 against the standard curve. Nonlinear regression analysis (curve fitting analysis) was performed by GraphPad Prism software version 9.0 (GraphPad Software Inc. San Diego, CA, USA)

4.6. Wound healing assay [55]

Huh7 cells at 5 × 10⁵ cells/well (2 mL) were seeded in completed DMEM medium in 12-well plates. Cells were incubated at 37 °C in the presence of 5% CO₂ for 24 h. The medium was removed from plates followed by scratching a wound with a sterile pipette tip at an angle about 30° in three parallel vertical lines then the wound was double washed with PBS. The wounded cell was treated with 2 mL of IC₅₀ concentration of the inhibitor diluted in the medium. Their cell migration was monitored with a microscope at 0, 24 and 48 h by calculated the cell repair percentage compared with control and Sorafenib, which is a positive control.

4.7. BrdU cell proliferative activity assay [56]

BrdU cell proliferative activity was performed by BrdU Cell Proliferation Assay kit (Cell signalling, 6813) according to the manufacturer's protocol. Huh7 cells at 4.5 × 10⁴ cells/200 µL were seeded into 96-well plate and incubated with Sorafenib at the concentration of 3 µM and 2 mM at 3, 6 and 12 µM for 0, 24 and 48 h then evaluated the absorbance at 450 nm by Thermo Scientific™ Multiskan™ GO Microplate Spectrophotometer.

Declaration of Competing Interest

The authors declared that there is no conflict of interest.

Acknowledgements

This research was financially supported by the Research Fund for DPST Graduate with First Placement (Grant Number 19/2558) from the Institute for the Promotion of Teaching Science and Technology (IPST), The Thailand Research Fund (RTA6280004), Department of Chemistry, Faculty of Science, Silpakorn University and Center of Excellence in Hepatitis and Liver Cancer, Department of Biochemistry, Faculty of Medicine, Chulalongkorn University.

Appendix A. Supplementary data

Supplementary data to this article can be found online at <https://doi.org/10.1016/j.bioorg.2021.104831>.

References

- [1] F. Bray, J. Ferlay, I. Soerjomataram, R.L. Siegel, L.A. Torre, A. Jemal, Global cancer statistics 2018: GLOBOCAN estimates of incidence and mortality worldwide for 36 cancers in 185 countries, *CA Cancer J. Clin.* 68 (2018) 394–424, <https://doi.org/10.3322/caac.21492>.
- [2] D.M. Parkin, F. Bray, J. Ferlay, P. Pisani, Global cancer statistics, 2002, *CA Cancer J. Clin.* 55 (2005) 74–108, <https://doi.org/10.3322/canjclin.55.2.74>.

- [3] H.O. Adami, A.W. Hsing, J.K. McLaughlin, D. Trichopoulos, D. Hacker, A. Ekblom, I. Persson, Alcoholism and liver cirrhosis in the etiology of primary liver cancer, *Int. J. Cancer* 51 (1992) 898–902, <https://doi.org/10.1002/ijc.2910510611>.
- [4] B. Charrez, L. Qiao, L. Hebbard, Hepatocellular carcinoma and non-alcoholic steatohepatitis: The state of play, *World J. Gastroenterol.* 22 (2016) 2494–2502, <https://doi.org/10.3748/wjg.v22.i8.2494>.
- [5] K.A. Steinmetz, J.D. Potter, Vegetables, fruit, and cancer I. Epidemiology, *Cancer Causes Control* 2 (1991) 325–357, <https://doi.org/10.1007/bf00051672>.
- [6] K. Rapp, J. Schroeder, J. Klenk, S. Stoehr, H. Ulmer, H. Concin, G. Diem, W. Oberaigner, S.K. Weiland, Obesity and incidence of cancer: a large cohort study of over 145,000 adults in Austria, *Br. J. Cancer* 93 (2005) 1062–1067, <https://doi.org/10.1038/sj.bjc.6602819>.
- [7] S.-C. Chuang, C. La Vecchia, P. Boffetta, Liver cancer: descriptive epidemiology and risk factors other than HBV and HCV infection, *Cancer Lett.* 286 (2009) 9–14.
- [8] E.R. Schiff, S.S. Lee, Y.C. Chao, S. Kew Yoon, F. Bessone, S.S. Wu, W. Kryczka, Y. Lurie, A. Gadano, G. Kitis, et al., Long-term treatment with entecavir induces reversal of advanced fibrosis or cirrhosis in patients with chronic hepatitis B, *Clin. Gastroenterol. Hepatol.* 9 (2011) 274–276, <https://doi.org/10.1016/j.cgh.2010.11.040>.
- [9] J. Balogh, D. Victor 3rd, E.H. Asham, S.G. Burroughs, M. Boktour, A. Saharia, X. Li, R.M. Ghobrial, H.P. Monsour Jr., Hepatocellular carcinoma: a review, *J. Hepatocell. Carcinoma* 3 (2016) 41–53, <https://doi.org/10.2147/JHC.S61146>.
- [10] J.-W. Jang, Y. Song, K.M. Kim, J.-S. Kim, E.K. Choi, J. Kim, H. Seo, Hepatocellular carcinoma-targeted drug discovery through image-based phenotypic screening in co-cultures of HCC cells with hepatocytes, *BMC Cancer* 16 (2016) 810.
- [11] S. Daher, M. Massarwa, A.A. Benson, T. Khoury, Current and Future Treatment of Hepatocellular Carcinoma: An Updated Comprehensive Review, *J. Clin. Transl. Hepatol.* 6 (2018) 69–78, <https://doi.org/10.14218/JCTH.2017.00031>.
- [12] A. Raza, G.K. Sood, Hepatocellular carcinoma review: current treatment, and evidence-based medicine, *World J. Gastroenterol.* 20 (2014) 4115–4127, <https://doi.org/10.3748/wjg.v20.i15.4115>.
- [13] F. Wang, W. Dai, Y. Wang, M. Shen, K. Chen, P. Cheng, Y. Zhang, C. Wang, J. Li, Y. Zheng, et al., The synergistic *in vitro* and *in vivo* antitumor effect of combination therapy with salinomycin and 5-fluorouracil against hepatocellular carcinoma, *PLoS ONE* 9 (2014), e97414, <https://doi.org/10.1371/journal.pone.0097414>.
- [14] P. Michl, S. Pauls, T.M. Gress, Evidence-based diagnosis and staging of pancreatic cancer, *Best Pract. Res. Clin. Gastroenterol.* 20 (2006) 227–251, <https://doi.org/10.1016/j.bpg.2005.10.005>.
- [15] Z. Zhang, B. Niu, J. Chen, X. He, X. Bao, J. Zhu, H. Yu, Y. Li, The use of lipid-coated nanodiamond to improve bioavailability and efficacy of sorafenib in resisting metastasis of gastric cancer, *Biomaterials* 35 (2014) 4565–4572.
- [16] W. Jeong, J.H. Doroshov, S. Kummur, US FDA approved oral kinase inhibitors for the treatment of malignancies, *Curr. Probl. Cancer* 37 (2013) 110–144.
- [17] P.T. White, M.S. Cohen, The discovery and development of sorafenib for the treatment of thyroid cancer, *Expert Opin. Drug Discov.* 10 (2015) 427–439, <https://doi.org/10.1517/17460441.2015.1006194>.
- [18] S. Wilhelm, C. Carter, M. Lynch, T. Lowinger, J. Dumas, R.A. Smith, B. Schwartz, R. Simantov, S. Kelley, Discovery and development of sorafenib: a multikinase inhibitor for treating cancer, *Nat. Rev. Drug Discovery* 5 (2006) 835–844, <https://doi.org/10.1038/nrd2130>.
- [19] M.B. Toaldo, V. Salvatore, S. Marinelli, C. Palamà, M. Milazzo, L. Croci, L. Venerandi, M. Cipone, L. Bolondi, F. Piscaglia, Use of VEGFR-2 targeted ultrasound contrast agent for the early evaluation of response to sorafenib in a mouse model of hepatocellular carcinoma, *Mol. Imaging Biol.* 17 (2015) 29–37.
- [20] J.M. Llovet, S. Ricci, V. Mazzaferro, P. Hilgard, E. Gane, J.F. Blanc, A.C. de Oliveira, A. Santoro, J.L. Raoul, A. Forner, et al., Sorafenib in advanced hepatocellular carcinoma, *N. Engl. J. Med.* 359 (2008) 378–390, <https://doi.org/10.1056/NEJMoa0708857>.
- [21] P. Wu, T.E. Nielsen, M.H. Clausen, FDA-approved small-molecule kinase inhibitors, *Trends Pharmacol. Sci.* 36 (2015) 422–439.
- [22] A.T. Weckslers, S.H. Hwang, J.Y. Liu, H.I. Wettersten, C. Morisseau, J. Wu, R. H. Weiss, B.D. Hammock, Biological evaluation of a novel sorafenib analogue, t-CUPM, *Cancer Chemother. Pharmacol.* 75 (2015) 161–171, <https://doi.org/10.1007/s00280-014-2626-2>.
- [23] L.S. Wood, Management of vascular endothelial growth factor and multikinase inhibitor side effects, *Clin. J. Oncol. Nurs.* 13 (Suppl) (2009) 13–18, <https://doi.org/10.1188/09.CJON.S2.13-18>.
- [24] M. Mannion, S. Raepfel, S. Claridge, N. Zhou, O. Saavedra, L. Isakovic, L. Zhan, F. Gaudette, F. Raepfel, R. Deziel, et al., N-(4-(6,7-Disubstituted-quinolin-4-yloxy)-3-fluorophenyl)-2-oxo-3-phenylimidazole dine-1-carboxamides: a novel series of dual c-Met/VEGFR2 receptor tyrosine kinase inhibitors, *Bioorg. Med. Chem. Lett.* 19 (2009) 6552–6556, <https://doi.org/10.1016/j.bmcl.2009.10.040>.
- [25] W. Zhan, Y. Li, W. Huang, Y. Zhao, Z. Yao, S. Yu, S. Yuan, F. Jiang, S. Yao, S. Li, Design, synthesis and antitumor activities of novel bis-aryl ureas derivatives as Raf kinase inhibitors, *Bioorg. Med. Chem.* 20 (2012) 4323–4329.
- [26] C.-r. Zhao, R.-q. Wang, G. Li, X.-x. Xue, Sun C-j, Qu X-j, Li W-b. Synthesis of indazole based diarylurea derivatives and their antiproliferative activity against tumor cell lines, *Bioorg. Med. Chem. Lett.* 23 (2013) 1989–1992.
- [27] Z. Liu, Y. Wang, H. Lin, D. Zuo, L. Wang, Y. Zhao, P. Gong, Design, synthesis and biological evaluation of novel thieno [3, 2-d] pyrimidine derivatives containing diaryl urea moiety as potent antitumor agents, *Eur. J. Med. Chem.* 85 (2014) 215–227.
- [28] M. Qin, S. Yan, L. Wang, H. Zhang, Y. Zhao, S. Wu, D. Wu, P. Gong, Discovery of novel diaryl urea derivatives bearing a triazole moiety as potential antitumor agents, *Eur. J. Med. Chem.* 115 (2016) 1–13.
- [29] M. Wang, S. Xu, H. Lei, C. Wang, Z. Xiao, S. Jia, J. Zhi, P. Zheng, W. Zhu, Design, synthesis and antitumor activity of Novel Sorafenib derivatives bearing pyrazole scaffold, *Bioorg. Med. Chem.* 25 (2017) 5754–5763, <https://doi.org/10.1016/j.bmc.2017.09.003>.
- [30] F. Chen, Y. Fang, R. Zhao, J. Le, B. Zhang, R. Huang, Z. Chen, J. Shao, Evolution in medicinal chemistry of sorafenib derivatives for hepatocellular carcinoma, *Eur. J. Med. Chem.* 179 (2019) 916–935, <https://doi.org/10.1016/j.ejmech.2019.06.070>.
- [31] M. Wang, S. Xu, C. Wu, X. Liu, H. Tao, Y. Huang, Y. Liu, P. Zheng, W. Zhu, Design, synthesis and activity of novel sorafenib analogues bearing chalcone unit, *Bioorg. Med. Chem. Lett.* 26 (2016) 5450–5454, <https://doi.org/10.1016/j.bmcl.2016.10.029>.
- [32] E.M. Gordon, N.S. Chawla, F.L. Hall, S.P. Chawla, A two decade review of approved drugs and drugs in development in the United States, *New Cancer Therapies for the 21st* (2015).
- [33] L.J. Scott, Lenvatinib: first global approval, *Drugs* 75 (2015) 553–560, <https://doi.org/10.1007/s40265-015-0383-0>.
- [34] E.S. Kim, Tivozanib: First Global Approval, *Drugs* 77 (2017) 1917–1923, <https://doi.org/10.1007/s40265-017-0825-y>.
- [35] Y. Tian, S. Yu, L. Cai, G. Gong, G. Wu, H. Qi, Y. Zhao, M. Qin, Synthesis and Antitumor Activity of Sorafenib Analogs Containing a Tetrazole Moiety, *Chem. Res. Chin. Univ.* 35 (2019) 41–46.
- [36] P. Alam, S.K. Chaturvedi, T. Anwar, M.K. Siddiqi, M.R. Ajmal, G. Badr, M. H. Mahmoud, R.H. Khan, Biophysical and molecular docking insight into the interaction of cytosine β-D arabinofuranoside with human serum albumin, *J. Lumin.* 164 (2015) 123–130.
- [37] J. Vallner, Binding of drugs by albumin plasma protein, *J. Pharm. Sci.* 66 (1977) 447–465.
- [38] S.G. Agalave, S.R. Maujan, V.S. Pore, Click chemistry: 1, 2, 3-triazoles as pharmacophores, *Chem. Asian J.* 6 (2011) 2696–2718.
- [39] S. Haider, M.S. Alam, H. Hamid, 1,2,3-Triazoles: scaffold with medicinal significance, *Inflamm. Cell Signal.* 1 (2014), e95.
- [40] C.S. Santos, R.J. de Oliveira, R.N. de Oliveira, J.C.R. Freitas, 1,2,3-Triazoles: general and key synthetic strategies, *Arkivoc* (2020).
- [41] H.C. Zhou, Y. Wang, Recent researches in triazole compounds as medicinal drugs, *Curr. Med. Chem.* 19 (2012) 239–280.
- [42] S. Palakachane, Y. Ketkaew, N. Chuaypen, P. Tangkijvanich, A. Suksamrarn, P. Limpachayaporn, The preliminary studies on the synthesis and the cytotoxicity towards HepG2 and Huh7 of a new series of sorafenib analogues: Replacement of aryl urea with a triazole ring. The 45th Congress on Science and Technology of Thailand, Mae Fah Luang University, Chiang Rai, Thailand, 2019.
- [43] B.-Y. Ryu, T. Emrick, Bisphenol-1, 2, 3-triazole (BPT) epoxies and cyanate esters: synthesis and self-catalyzed curing, *Macromolecules* 44 (2011) 5693–5700.
- [44] G. Munagala, K.R. Yempalla, S. Singh, S. Sharma, N.P. Kalia, V.S. Rajput, S. Kumar, S.D. Sawant, I.A. Khan, R.A. Vishwakarma, Synthesis of new generation triazolyl- and isoxazolyl-containing 6-nitro-2, 3-dihydroimidazo[4,5-b]pyridine agents: *in vitro*, structure–activity relationship, pharmacokinetics and *in vivo* evaluation, *Org. Biomol. Chem.* 13 (2015) 3610–3624.
- [45] Y-y Wang, J-z Liu, X-y Yu, D-z Yang, L-n Zhang, G-s Zhao, Design and synthesis of hydrazine and oxadiazole-containing derivatives of Sorafenib as antitumor agents, *Chem. Res. Chin. Univ.* 29 (2013) 454–459.
- [46] L. Tan, Z. Zhang, D. Gao, J. Luo, Z.-C. Tu, Z. Li, L. Peng, X. Ren, K. Ding, 4-Oxo-1, 4-dihydroquinoline-3-carboxamide derivatives as new Axl kinase inhibitors, *J. Med. Chem.* 59 (2016) 6807–6825.
- [47] C. Nagel, S. Armeanu-Ebinger, A. Dewerth, S.W. Warmann, J. Fuchs, Anti-tumor activity of sorafenib in a model of a pediatric hepatocellular carcinoma, *Exp. Cell Res.* 331 (2015) 97–104.
- [48] S.S. Zhang, Y.H. Ni, C.R. Zhao, Z. Qiao, H.X. Yu, L.Y. Wang, J.Y. Sun, C. Du, J. H. Zhang, L.Y. Dong, et al., Capsaicin enhances the antitumor activity of sorafenib in hepatocellular carcinoma cells and mouse xenograft tumors through increased ERK signaling, *Acta Pharmacol. Sin.* 39 (2018) 438–448, <https://doi.org/10.1038/aps.2017.156>.
- [49] M. Cervello, D. Bachvarov, N. Lampiasi, A. Cusimano, A. Azzolina, J.A. McCubrey, G. Montalto, Molecular mechanisms of sorafenib action in liver cancer cells, *Cell Cycle* 11 (2012) 2843–2855, <https://doi.org/10.4161/cc.21193>.
- [50] M.A. Rodríguez-Hernández, R. Chapresto-Garzón, M. Cadenas, E. Navarro-Villarán, M. Negrete, M.A. Gómez-Bravo, V.M. Victor, F.J. Padillo, J. Muntané, Differential effectiveness of tyrosine kinase inhibitors in 2D/3D culture according to cell differentiation, p53 status and mitochondrial respiration in liver cancer cells, *Cell Death Dis.* 11 (2020) 1–10.
- [51] S. Thongnest, J. Boonsombat, H. Prawat, C. Mahidol, S. Ruchirawat, Ailanthus AG and nor-lupane triterpenoids from *Ailanthus triphysa*, *Phytochemistry* 134 (2017) 98–105.
- [52] C. Wang, H. Jin, D. Gao, C. Liefink, B. Evers, G. Jin, Z. Xue, L. Wang, R. L. Beijersbergen, W. Qin, Phospho-ERK is a biomarker of response to a synthetic lethal drug combination of sorafenib and MEK inhibition in liver cancer, *J. Hepatol.* 69 (2018) 1057–1065.
- [53] K.-C. Hsu, Y.-F. Chen, S.-R. Lin, J.-M. Yang, iGEMDOCK: a graphical environment of enhancing GEMDOCK using pharmacological interactions and post-screening analysis, *BMC Bioinf.* 12 (2011) S33.
- [54] W. Gao, A.P.-C. Chen, C.-H. Leung, E.A. Gullen, A. Fürstner, Q. Shi, L. Wei, K.-H. Lee, Y.-C. Cheng, Structural analogs of tylophora alkaloids may not be functional analogs, *Bioorg. Med. Chem. Lett.* 18 (2008) 704–709.
- [55] S. Elswa, X. Zheng, N.B.R. Vittar, X. Gai, M.G. Fernandez-Barrera, C.D. Moser, C. Hu, L.L. Almada, A.L. McCleary-Wheeler, A.M. Vrabel, The Transcription Factor GLI1 Mediates TGFβ1 Driven EMT in Hepatocellular Carcinoma via a SNAI1-Dependent Mechanism, *PLoS ONE* (2012).

- [56] T. Song, C. Wang, C. Guo, Q. Liu, X. Zheng, Pentraxin 3 overexpression accelerated tumor metastasis and indicated poor prognosis in hepatocellular carcinoma via driving epithelial-mesenchymal transition, *J. Cancer* 9 (2018) 2650–2658, <https://doi.org/10.7150/jca.25188>.
- [57] R.G. Schmidt, E.K. Bayburt, S.P. Latschaw, J.R. Koenig, J.F. Daanen, H. A. McDonald, B.R. Bianchi, C.M. Zhong, S. Joshi, P. Honore, et al., Chroman and tetrahydroquinoline ureas as potent TRPV1 antagonists, *Bioorg. Med. Chem. Lett.* 21 (2011) 1338–1341, <https://doi.org/10.1016/j.bmcl.2011.01.056>.
- [58] C. Ferroni, A. Pepe, Y.S. Kim, S. Lee, A. Guerrini, M.D. Parenti, A. Tesei, A. Zamagni, M. Cortesi, N. Zaffaroni, et al., 1,4-Substituted Triazoles as Nonsteroidal Anti-Androgens for Prostate Cancer Treatment, *J. Med. Chem.* 60 (2017) 3082–3093, <https://doi.org/10.1021/acs.jmedchem.7b00105>.
- [59] S. Kotha, D. Bansal, R.V. Kumar, Synthesis of symmetrical and unsymmetrical trisubstituted benzene derivatives through ring-closing alkyne metathesis strategy and depropargylation with various catalysts, *Indian J. Chem. B* 48B (2009) 225–230.
- [60] F. Khurshid, M. Jeyavelan, K. Takahashi, M.S.L. Hudson, S. Nagarajan, Aryl fluoride functionalized graphene oxides for excellent room temperature ammonia sensitivity/selectivity, *RSC Adv.* 8 (2018) 20440–20449, <https://doi.org/10.1039/c8ra01818a>.
- [61] V.S.P.R. Lingam, R. Vinodkumar, K. Mukkanti, A. Thomas, B. Gopalan, A simple approach to highly functionalized benzo[b]furans from phenols and aryl iodides via aryl propargyl ethers, *Tetrahedron Lett.* 49 (2008) 4260–4264, <https://doi.org/10.1016/j.tetlet.2008.04.150>.
- [62] J. Kong, T. Meng, J. Su, A Unique Synthesis of 5, 8-Difluoro-2 H-chromene Using Silicone Oil as a Solvent, *Org. Process Res. Dev.* 19 (2015) 681–683.
- [63] I. Volchkov, D. Lee, Asymmetric Total Synthesis of (-)-Amphidinolide V through Effective Combinations of Catalytic Transformations, *J. Am. Chem. Soc.* 135 (2013) 5324–5327, <https://doi.org/10.1021/ja401717b>.
- [64] K. Lu, L.D. Cai, X. Zhang, G.D. Wu, C.J. Xu, Y.F. Zhao, P. Gong, Design, synthesis, and biological evaluation of novel substituted benzamide derivatives bearing a 1,2,3-triazole moiety as potent human dihydroorotate dehydrogenase inhibitors, *Bioorg. Chem.* 76 (2018) 528–537, <https://doi.org/10.1016/j.bioorg.2017.12.025>.
- [65] D. Prasad, N. Aggarwal, R. Kumar, M. Nath, Synthesis of novel heteroarenes based [1,2,3]-triazoles via click chemistry and their evaluation for antibacterial activity, *Indian J. Chem. B* 51B (2012) 731–738.
- [66] J. Chen, L. Ma, R. Zhang, J. Tang, H. Lai, J. Wang, G. Wang, Q. Xu, T. Chen, F. Peng, Semi-Synthesis and Biological Evaluation of 1, 2, 3-Triazole-Based Podophyllotoxin Congeners as Potent Antitumor Agents Inducing Apoptosis in HepG2 Cells, *Arch. Pharm.* 345 (2012) 945–956.
- [67] M. Irfan, B. Aneja, U. Yadava, S.I. Khan, N. Manzoor, C.G. Daniliuc, M. Abid, Synthesis, QSAR and anticandidal evaluation of 1,2,3-triazoles derived from naturally bioactive scaffolds, *Eur. J. Med. Chem.* 93 (2015) 246–254, <https://doi.org/10.1016/j.ejmech.2015.02.007>.
- [68] Y. Tsuzuki, T.K.N. Nguyen, D.R. Garud, B. Kuberan, M. Koketsu, 4-Deoxy-4-fluoroxyloside derivatives as inhibitors of glycosaminoglycan biosynthesis, *Bioorg. Med. Chem. Lett.* 20 (2010) 7269–7273, <https://doi.org/10.1016/j.bmcl.2010.10.085>.
- [69] J. Li, F. Yang, Y.T. Ma, K. Ji, Gold (III)-Catalyzed Intermolecular Oxidation-Cyclization of Ynones: Access to 4-Substituted Chroman-3-ones, *Adv. Synth. Catal.* 361 (2019) 2148–2153.
- [70] R. Balasubramanian, K. Kumutha, M. Sarojadevi, Mechanical, thermal and electrical properties of polyimides containing 1,2,3-triazole ring prepared by click reaction, *Polym. Bull.* 73 (2016) 309–330.
- [71] D.A. Volpe, S.S. Hamed, L.K. Zhang, Use of different parameters and equations for calculation of IC₅₀ values in efflux assays: potential sources of variability in IC₅₀ determination, *The AAPS journal* 16 (2014) 172–180.